www.nature.com/npp

American College of Neuropsychopharmacology

REVIEW ARTICLE OPEN

Check for updates

Synaptic changes in psychiatric and neurological disorders: state-of-the art of in vivo imaging

Oliver Howes[1,2,3]✉, Julia Marcinkowska[1], Federico E. Turkheimer[4] and Richard Carr[1,2,3]

Synapses are implicated in many neuropsychiatric illnesses. Here, we provide an overview of in vivo techniques to index synaptic markers in patients. Several positron emission tomography (PET) tracers for synaptic vesicle glycoprotein 2 A (SV2A) show good reliability and selectivity. We review over 50 clinical studies including over 1700 participants, and compare findings in healthy ageing and across disorders, including addiction, schizophrenia, depression, posttraumatic stress disorder, and neurodegenerative disorders, including tauopathies, Huntington's disease and α-synucleinopathies. These show lower SV2A measures in cortical brain regions across most of these disorders relative to healthy volunteers, with the most well-replicated findings in tauopathies, whilst changes in Huntington's chorea, Parkinson's disease, corticobasal degeneration and progressive supranuclear palsy are predominantly subcortical. SV2A PET measures are correlated with functional connectivity across brain networks, and a number of other measures of brain function, including glucose metabolism. However, the majority of studies found no relationship between grey matter volume measured with magnetic resonance imaging and SV2A PET measures. Cognitive dysfunction, in domains including working memory and executive function, show replicated inverse relationships with SV2A measures across diagnoses, and initial findings also suggest transdiagnostic relationships with mood and anxiety symptoms. This suggests that synaptic abnormalities could be a common pathophysiological substrate underlying cognitive and, potentially, affective symptoms. We consider limitations of evidence and future directions; highlighting the need to develop postsynaptic imaging markers and for longitudinal studies to test causal mechanisms.

Neuropsychopharmacology (2025) 50:164–183; https://doi.org/10.1038/s41386-024-01943-x

INTRODUCTION

Most complex brain functions rely on synapses [1]. Unsurprisingly, therefore, synaptic alterations are implicated in many neurological and psychiatric disorders [2, 3]. Synaptic markers have historically been measured postmortem, often utilising immunofluorescence to study the density of synaptic vesicle proteins [4]. However, synaptic changes may occur after death [5], and cause of death may affect synapses [6]. Furthermore, it is not possible to study changes during the course of the disorder or relate them to the development of clinical sequelae in the same individual in postmortem studies. These issues highlight the need for techniques for in vivo investigation of synapses in the brain to enable determination of relationships between synaptic markers and clinical features of illness, and how they change with time. The last decade has seen the development of positron emission tomography (PET) imaging techniques to quantify synaptic proteins, providing the most direct in vivo measures of synaptic markers for use in humans available to date [7]. These PET methods are now being used to study synaptic protein levels in a number of neuropsychiatric disorders, which makes it timely to consider progress to date and future avenues of investigation. In view of this, we first provide an overview of synaptic organisation and the elements indexed by current neuroimaging methods. Following this, we discuss PET, and the tracers that have been developed to target synaptic proteins. We then review the findings to date in neuropsychiatric disorders, comparing the regions and degree of alterations, and reviewing convergent transdiagnostic SV2A findings in cognition and relationships with other neuroimaging measures. These aspects have not been comprehensively covered by previous reviews of SV2A imaging [8–10] to our knowledge. Finally, we consider the limitations of current approaches and next steps.

OVERVIEW OF THE SYNAPSE

The synapse comprises a presynaptic terminal, the synaptic cleft and the postsynaptic density (Fig. 1a). In the presynaptic terminal, calcium influx induced by incoming action potentials causes synaptic vesicles to fuse with the presynaptic terminal membrane and release the neurotransmitter into the synaptic cleft (Fig. 1b). The neurotransmitter diffuses across the cleft and binds to receptors on the postsynaptic density [11]. The binding of neurotransmitter can produce diverse effects, including excitation, inhibition and induction of synaptic plasticity [12]. Consequently, the synapse is the core unit of information processing in the brain [13].

[1]Department of Psychosis Studies, Institute of Psychiatry, Psychology and Neuroscience, King's College London, London, England. [2]South London & the Maudsley NHS Trust, London, England. [3]London Institute of Medical Sciences, London, England. [4]Department of Neuroimaging, Institute of Psychiatry, Psychology and Neuroscience, King's College London, London, England. ✉email: oliver.howes@kcl.ac.uk

Received: 27 March 2024 Revised: 3 July 2024 Accepted: 19 July 2024
Published online: 12 August 2024

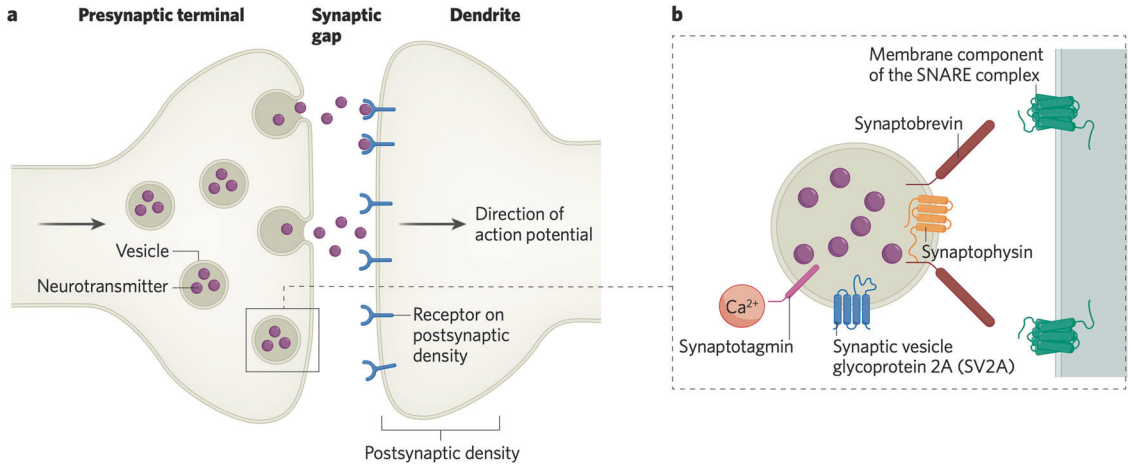

Fig. 1 Structure of a typical synapse and synaptic vesicle. a Overview of the synapse, showing the presynaptic terminal with vesicles containing neurotransmitter, synaptic gap, and the postsynaptic density with neurotransmitter binding to receptors. Action potentials (arrow) trigger vesicular fusion with the presynaptic membrane to release neurotransmitter (**b**), which then diffuses across the synaptic gap to bind to receptors in the post-synaptic density. **b** Representation of a vesicle primed for fusion with the presynaptic membrane, showing key vesicle proteins. SNARE soluble *N*-ethylamide-sensitive factor attachment protein receptor complex.

Synaptic vesicles are complex structures, containing protein machinery for packaging vesicles with neurotransmitter [14], responding to calcium influx into the presynaptic terminal to initiate exocytosis, mediated by synaptotagmin, a calcium sensor [15], and for fusing with the synaptic terminal membrane, mediated by the soluble *N*-ethylamide-sensitive factor attachment protein receptor (SNARE) complex of proteins. The SNARE complex comprises a membrane component and the vesicle protein synaptobrevin [16]. Other key proteins mediating these processes include synaptophysin and synaptic vesicle glycoprotein 2 A (SV2A), both of which are thought to control the trafficking of other vesicle proteins such as synaptobrevin and synaptotagmin respectively (Fig. 1B) [8, 17]. Postmortem studies often use immunolabelling of these synaptic proteins [18], particularly synaptophysin, while current PET methods for synaptic imaging use tracers that bind to SV2A. SV2A is, as far as is known, ubiquitously expressed in synapses, making it a good marker of synapses [19]. Visualisation of the distribution of synaptophysin and SV2A shows that the two proteins colocalise in the synapse, at least in mouse brain, suggesting alignment between the primary targets measured with in vitro and in vivo methods respectively [20].

SYNAPTIC IMAGING

Background

Synaptic imaging studies using PET typically estimate one of four outcome measures; volume of distribution (V_T), distribution volume ratio (DVR), standardised uptake value ratio (SUVR) and nondisplaceable binding potential (BP_{ND}). A detailed description of outcome measures is beyond the scope of this review, however a brief summary is present in the Supplementary Materials, and further detail can be found in previous reviews on the subject [7, 21].

The ideal tracer for investigating synaptic density requires a target present in all synapses, but not expressed in other cellular components. While not perfect as a target, synaptic vesicle glycoprotein 2A (SV2A) is a protein that approaches this ideal and for which there are PET tracers available for human imaging [7]. SV2A is a member of the SV2 family of transmembrane vesicle proteins [8], present in presynaptic terminals (Fig. 1) with no evidence for expression in the postsynaptic density. A number of tracers that bind to SV2A with high affinity and selectivity have been developed, summarised in Table 1. One of the first produced was [^{11}C]LEV, based on the SV2A modulator levetiracetam [22]. However, [^{11}C]LEV has not been used for human studies, due to poor brain uptake [23]. Three other tracers with more rapid brain penetrance have been developed: [^{11}C]UCB-A, [^{18}F]UCB-H, and [^{11}C]UCB-J [24]. The inferior brain uptake of [^{11}C]UCB-A relative to the other UCB tracers [25] meant it has not proceeded to human studies [26].

Of the UCB tracers, [^{11}C]UCB-J has higher affinity for SV2A [27] (Table 1) and higher specific signal than [^{18}F]UCB-H [27]. Test-retest variability was ≤10% for all the tracers where it has been examined, indicating low within-subject variability (Table 1). These test-retest studies have generally been over 1–7 days. However, one study conducted [^{11}C]UCB-J PET scans performed four weeks apart [28] showing comparable low variability to shorter-term studies in three outcome measures, with volume of distribution, distribution volume ratio and nondisplaceable binding potential in total grey matter (GM) showing test-retest values of $-7.7 \pm 4.3\%$, $-6.6 \pm 6.1\%$, and $-8.2 \pm 9.6\%$ respectively.

The SynVesT tracers are fluorinated analogues of UCB-J [29]. This allows radiofluorination into [^{18}F] tracers, a favourable practical factor for clinical applications, as the slower decay of the tracer allows it to be produced off-site and transported to imaging centres without synthesis facilities. They are also less lipophilic, which may decrease nonspecific binding [30]. However, they are rapidly broken down, with <50% of the parent molecule present at 30 min post-injection [31]. They have since been used in human research [32, 33], with [^{18}F]SynVesT-1 showing higher BP_{ND} compared to [^{11}C]UCB-J and very rapid kinetics [10, 34, 35]. [^{18}F]SynVesT-2 showed lower uptake than [^{18}F]SynVesT-1 and [^{11}C]UCB-J, with mean BP_{ND} values 42% and 24% lower than these respectively in direct comparison [30], meaning it will probably have lower sensitivity to pick up small changes in SV2A levels than the other tracers.

A seventh tracer, [^{18}F]SDM-16, was developed in 2021, based on the molecular structure of [^{11}C]UCB-A [31], designed to overcome the metabolic lability of other [^{18}F] tracers. It shows the highest affinity for SV2A, measured in rhesus macaques, and comparable BP_{ND} to other tracers (Table 1), but has not yet been used in humans.

In vivo selectivity of SV2A PET Tracers for SV2a

Blocking studies have been used to evaluate the specificity of PET tracers to SV2A. These involve PET scans using the tracer before and after administration of a drug which binds to the SV2A

Table 1. Summary of characteristics of tracers targeting SV2A.

Tracer	Affinity for SV2A (K_i, nM)	Measured BP_{ND}[a] (grey matter)	T_{max}	First Used in Humans	Test-retest variability (V_T)
[^{11}C]LEV	NI	NI	NI	Not used	NI
[^{11}C]UCB-A	1.2 [152]	NI	65 mins [25]	Not used	NI
[^{11}C]UCB-J	2.6 [152], 1.5 [153]	1.85–3.7 [35], 2.2–3.7 [30]	10–25 mins [35]	2016 [47]	3–9%; ICC > 0.6 [154]
[^{18}F]UCB-H	6.8 [152], 9 [153]	<1 [30]	10 mins [155] (NHP)	2015 [156]	10% [155] (NHP)
[^{18}F]SynVesT-1	3.1 [152], 2.2 [153]	2.4–4.3 [35], 2.8–4.6 [30]	5–20 mins [35]	2021 [35]	<9% [34]
[^{18}F]SynVest-2	9.6 [152]	1.6–3.0 [30]	7 mins (reported in thalamus and putamen only) [157], 7 mins (dlPFC and putamen only) [30]	2020 [30]	5.5% [157], 4.7–7.2% [29]
[^{18}F]SDM-16	0.9 [31] (NHP)	2.8 [31] (NHP)	NI	Not used in humans	7% [31] (NHP)

CSO centrum semiovale, *dlPFC* dorsolateral PFC, *ICC* interclass correlation coefficient (given where reported), *NHP* non-human primates, *SV2A* synaptic vesicle glycoprotein 2A, V_T volume of distribution, BP_{ND} binding potential, T_{max} time to maximum concentration in the brain, *NI* no information.
[a]Studies use the CSO to estimate BP_{ND}, which may not be a true reference region (see Limitations Section). As such this is not a true value of BP_{ND}.

Table 2. Results from blocking studies following administration of the SV2A modulator levetiracetam.

Tracer	Change in V_T following administration of different doses levetiracetam (% reduction, excluding centrum semiovale)					
	10 mg/kg (59% SV2A occupancy [26])	20 mg/kg (82.5–85.3% SV2A occupancy [35])	30 mg/kg (90% SV2A occupancy [26])	50 mg/kg (97.4% SV2A occupancy [158])	100 mg/kg (SV2A occupancy unknown)	200 mg/kg (100% SV2A occupancy [158]
[^{11}C]LEV	NI	NI	NI	NI	NI	NI
[^{11}C]UCB-A	NI	NI	NI	NI	NI	NI
[^{11}C]UCB-J	41.0–60.4 [26] (NHP)	55.2–67.7 [35] (humans)	58.3–78.3 [26] (NHP)	74.7–78.7 [158] (mice)	NI	84.1–86.7 [158] (mice)
[^{18}F]UCB-H	46.2 [159], 25.7–36.8 [43] (rats)	NI	NI	NI	34.4–55.8 [43] (rats)	NI
[^{18}F]SynVesT-1	NI	64.7–76.2 [35] (humans)	NI	60.6–78.6 [160] (mice)	NI	73.2–89.5 [160] (mice)
[^{18}F]SynVest-2	NI	65.0–70.6% (humans) [29]	NI	NI	NI	NI
[^{18}F]SDM-16	NI	NI	57% [31] (NHP)	NI	NI	NI

Data presented show the reduction in V_T in the post-dose PET scan compared to the baseline scan. In tracers which have higher selectivity for the SV2A protein, a greater proportion of that tracer will be in competition with levetiracetam at the protein, and therefore these will show greater V_T reductions in the post-dose scan. Data from different doses of levetiracetam are presented to allow comparison. Higher doses of levetiracetam are expected to occupy a greater proportion of SV2A protein, thus leading to a greater difference between baseline and post-dose V_T.
NHP non-human primates, *NI* no information, *SV2A* synaptic vesicle glycoprotein 2A.

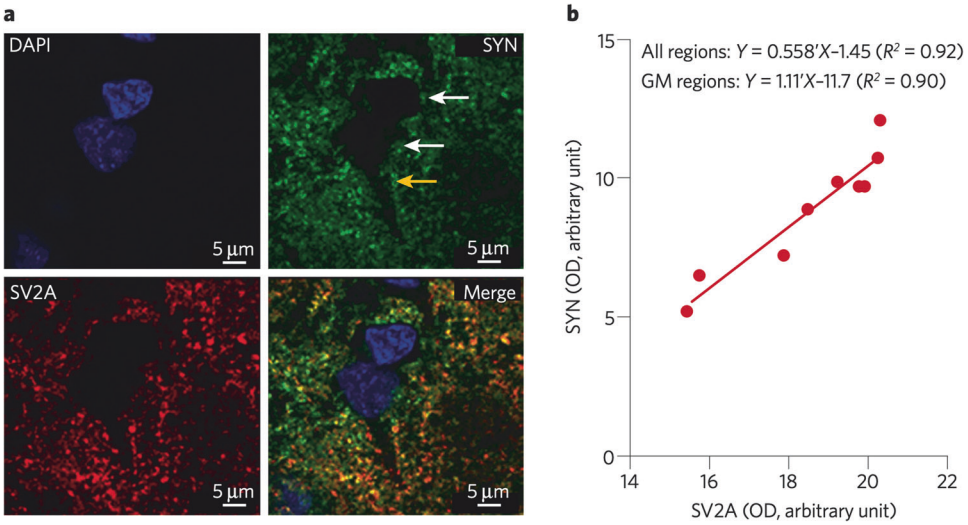

Fig. 2 Colocalisation of SV2A and synaptophysin in the baboon brain. a High-power confocal microscopy of 4′,6-diamidino-2-phenylindole (DAPI), synaptophysin (SYN), and synaptic vesicle glycoprotein 2A (SV2A) in the grey matter of the baboon brain. Labelling for SYN and SV2A is evident as punctate staining in the neuropil, particularly surrounding neuronal cell bodies and proximal dendrites (yellow arrow), but absent in neuronal cell bodies (white arrows). Nuclei are indicated by the DAPI stain in blue. **b** Correlation between in vitro SV2A and in vitro SYN density in grey matter regions determined using Western blot analyses. Data are nine brain regions. Figure and legend reproduced from Finnema et al. with permission (2016) [47]. GM grey matter, OD optical density.

protein, thus competing with the tracer. Tracers which show a larger decrease between scans are considered more selective [36]. However, even with perfect blocking, residual signal will remain due to nonspecific binding of the tracer, for example to lipids or other macromolecular cellular components [37]. Most such studies use levetiracetam, which has a moderate affinity for human SV2A (K_i: 6.1–8 µM) [38, 39]. While it shows negligible binding at the SV2 isoforms SV2B and SV2C [22], it has also been shown to bind to N-type voltage gated calcium channels [40] and AMPA receptors [41], although its affinity at these sites has not been reported.

Results from blocking studies are presented in Table 2. Whilst direct comparisons are complicated by studies being performed in different species, [^{11}C]UCB-J shows higher displacement at 30 mg/kg levetiracetam than [^{18}F]UCB-H at 100 mg/kg, and is roughly on-par with [^{18}F]SynVesT-1 at 200 mg/kg dose. [^{18}F]SynVesT-1 may slightly outperform [^{11}C]UCB-J at a 20 mg/kg dose in humans, showing higher displacement. One study has been performed with [^{18}F]SynVest-2, showing comparable reductions in V_T to [^{18}F]SynVesT-1 following 20 mg/kg levetiracetam [29]. No levetiracetam blocking data were found for [^{11}C]UCB-A or [^{11}C]LEV. Brivaracetam, another SV2A modulator shows higher affinity for the protein (K_i = 225 nM) than levetiracetam [42] and strong evidence of selectivity, with no specific binding observed in SV2A knockout mice [42]. It has been used in one blocking study [25] showing a ~75% decrease in whole-brain [^{11}C]UCB-A SUV following brivaracetam administration in mice.

In vitro studies have also been conducted with [^{11}C]UCB-J, finding a 10-fold greater selectivity for human SV2A over SV2C and a 100-fold greater selectivity over SV2B [27], however such studies have not been performed with other tracers. In vitro screening of both [^{11}C]UCB-J and [^{18}F]UCB-H revealed no significant activity (<50% inhibition at 10 µM) at a standard panel of receptors, ion channels and enzymes, including >55 potential targets [27, 43].

Validation Studies with SV2A PET Tracers

One key target for validation of these tracers is showing a clear relationship between SV2A tracer binding and established measures of synaptic density. Animal models provide evidence that SV2A tracers can detect synaptic loss, and are sensitive to change. For example, significant reductions in [^{11}C]UCB-J [44] and [^{18}F]SDM-16 [45] SUVR were detected in the hippocampus of the APP/PS1 mouse model of Alzheimer's dementia (AD), in which an independent ultramicroscopy study showed significant hippocampal synaptic degeneration [46]. Interestingly, a baboon study investigating both synaptophysin immunolabelling and [^{11}C]UCB-J V_T showed a very close correlation between V_T and synaptophysin immunofluorescence [47], providing cross-validation between the PET measure and one of the most widely used ex vivo synaptic markers (Fig. 2). While promising, this study was performed only on a single animal. Only one other similar study has been performed, which examined relationships between SV2A autoradiography using [^{3}H]UCB-J and synaptophysin mRNA levels, finding no correlation [48], however these authors did not look at synaptophysin protein levels. These issues, among others, are discussed in the Limitations section.

Another important issue is whether SV2A PET measures are affected by synaptic activity. To investigate this, Smart et al. [49] studied [^{11}C]UCB-J V_T and BP_{ND} in 7 healthy volunteers during visual stimulation, finding that, while influx of the tracer to visual cortex correlated with the functional magnetic resonance imaging (fMRI) blood oxygen-level dependent (BOLD) response, there was no change to [^{11}C]UCB-J V_T or BP_{ND}, indicating that these are likely stable measures and independent of acute changes in cortical activity.

In conclusion, of the four PET tracers currently used in clinical research which target SV2A, [^{11}C]UCB-J and [^{18}F]SynVesT-1 show the best properties. The following sections consider human findings using these tracers and their implications for understanding neuropsychiatric disorders.

SV2A FINDINGS IN VIVO

Healthy aging

Five cross-sectional studies have used [^{11}C]UCB-J PET to investigate relationships between SV2A levels and age in healthy participants (Table 3, Supplementary Table 2). Studies using V_T as an outcome consistently show lower cortical tracer uptake correlating with increasing age, particularly in the caudate nucleus [50, 51] and prefrontal cortex (PFC) [52]. As Table 3 shows, findings are less clear cut where SUVR is the outcome, with smaller [53] or non-significant [54] effects, although studies generally show lower

Table 3. Results from studies of SV2A PET in healthy participants from studiesshowing reductions in SV2A measures associated ageing.

Diagnosis	Reference	Comparison	Significant differences in SV2A PET measures (% difference, effect size or correlation coefficient)
HC	Andersen [98]	Old vs young SUVR	Nil significant
	Fang [52]	Correlation of age with SUVR	Greater age correlated with lower SUVR in mPFC (r = −0.37)
	Mansur [50, 142]	Correlation of age with V_T/f_p	Greater age correlated with lower V_T/f_p in CN ($\Delta V_T/f_p$ −1.31/year)
	Michiels [53]	Old vs young SUVR	↓ CN (1.7% RPD), ↓ CS
	Toyonaga [51]	HC (age-related) BP_F	↓ CN (3.6% RPD), ↓ CS (2.1% RPD), ↓ mOC (3.4% RPD)

One study of healthy controls also compared SV2A measures in escitalopram vs placebo (see supplementary Table S2), however is not included here as no significant differences were reported. If both PVC and non-PVC results were available, then only PVC were reported in the table. ↓=lower SV2A PET value in the region indicated. Nonsignificant findings are not reported, but full data can be accessed here GitHub.
r correlation coefficient, *BPf* free binding potential, *CN* caudate nucleus, *CS* centrum semiovale, *m* medial, *OC* occipital cortex, *RPD* reduction per decade, *SUVR* standardised uptake value ratio.

Box 1. Advantages and limitations of different pet outcome measures

SUVR: SUV is the ratio of tissue radioactivity concentration to injected dose divided by body weight. SUVR, or SUV ratio between an ROI and reference region [7], is generally best suited for metabolic tracers where uptake is almost irreversible. For tracers with reversible kinetics, radioactivity in a limited time-window is sensitive to the tracer clearance from tissue, hence strongly dependent on the start and end of the acquisition. SUVR does not require arterial blood sampling (ABS), long PET scans to acquire dynamic images, or complex modelling. However, it is not quantitative, and because it does not model the tracer input function, regional differences in tracer delivery are unaccounted for, increasing sensitivity to individual differences in tracer kinetics [65]. SUVR also requires a reference region in order to normalise for nonspecific binding, which relies on there being a brain region with certain properties, which may not be the case in synaptic PET imaging (see Limitations).

V_T: V_T is the estimate of the ratio between plasma and tissue radioactivity at equilibrium. V_T is obtained through the dynamic measurement of both plasma and tissue radioactive concentrations after a tracer bolus injection and use of a kinetic model, reducing the impact of subject variability in tracer delivery and clearance versus SUVR. A key advantage is that it is quantitative. However, this requires an arterial input function (AIF), increasing subject burden, costs, and analysis complexity. It also requires measurement of the plasma free fraction of tracer, f_p, which can introduce additional noise into measurements [142], particularly where f_p differs between subjects. In addition, V_T does not differentiate between displaceable and nondisplaceable binding, which may increase noise, particularly where there is between-subject variability in nondisplaceable uptake.

DVR: DVR is the ratio of V_T between the ROI and a reference region. If the reference region does not express the tracer target, then V_T here can be assumed to reflectnonspecific binding and free tracer in the reference region. DVR reduces variability in estimation of the AIFs [142]. However, as with SUVR, this assumes that the reference region is a true reference region, which may not always be the case (see Limitations) [59]. The quality of the reference region has large effects on the accuracy of results. Use of a reference region that exhibits specific binding of tracer will over-correct uptake estimates in the ROI, reducing the accuracy of a DVR study to detect changes.

BP_{ND}: BP_{ND} is calculated using the ratio of specific to nondisplaceable volume of distribution [21]. The major advantages of BP_{ND} include its versatility, as it can be calculated both using an AIF from V_T estimates, providing an outcome measure equalling DVR-1 [7], or using a simplified reference tissue model (SRTM) which is used to estimate the input function from the reference without ABS [161]. The former approach carries the same limitations as DVR. However the latter approach may slightly underestimate uptake compared to DVR [28], and relies on several assumptions which can bias BP_{ND} results in either direction while misleadingly retaining a good fit for the model if not met [59].

values in older age. Complicating interpretation of the SUVR studies is the finding of a positive correlation between [^{11}C]UCB-J SUV in the centrum semiovale (CSO) and age (Table 3), which may lead to underestimation of tracer binding in the rest of the brain in older participants where CSO is used as a reference region. This, along with other limitations of SUVR as a semi-quantitative outcome measure (Box 1, Limitations Section), may explain why changes are not consistently seen in SUVR studies (Table 3). Further work is needed to clarify these findings in SUVR studies, and longitudinal studies would be useful to identify within-subject changes in PET measures over time.

Schizophrenia

Four [^{11}C]UCB-J PET studies have been performed in people with schizophrenia (Table 4, Supplementary Table 3) [55–58]. The two studies in patients with chronic illness, using V_T [55] and BP_{ND}, derived from V_T estimates [58] respectively, both showed lower [^{11}C]UCB-J uptake in the cortex and hippocampus, with similar effect sizes. In contrast, findings early in the course of illness were not so consistent. Yoon et al. [57] found significantly lower [^{11}C]UCB-J BP_{ND}, derived from reference tissue estimates, in several cortical and subcortical regions (Table 4) relative to controls, while Onwordi et al. [56], found no significant difference in V_T but did find significantly lower [^{11}C]UCB-J DVR in the temporal lobe versus controls. Significant negative correlations between frontal tracer uptake and positive symptoms were found in two of the four studies, one each studying early-illness [57] and chronic [58] cohorts, with a similar trend detected in Onwordi's study investigating early-illness [56] (Table 7).

The use of outcome measures differed between the studies. Onwordi et al. used V_T measures and derived DVR using them (see Supplementary), while Yoon et al. used BP_{ND} derived from the SRTM, without ABS. In the latter case, the CSO was used as a reference region, which may violate two of the assumptions required for the model [59], namely that the reference region is devoid of specific binding, and that the CSO and regions of interest have the same nondisplaceable uptake (see Limitations). Both of these violations have been shown in computational models to negatively bias BP_{ND} results, with a greater negative bias at lower BP_{ND} [59], which could thus inflate the difference in measured BP_{ND} between patients and controls. Given this inconsistency and the possibility that differences may be inflated using BP_{ND}, further studies reporting V_T as well as other outcome measures are needed in early course patients.

Another consideration is that, with the exception of the study by Onwordi et al. (2023), most of the patients in these studies were taking antipsychotic medication. However, administration of the antipsychotics haloperidol and olanzapine to rats for 28 days resulted in no difference in SV2A on markers [55, 60] relative to vehicle-treated rats. Similar results were found on in vitro measures such as neuroligin puncta density [60] and synaptophysin immunoreactivity [61]. In contrast, synaptic density, as observed with microscopy, has been found to be higher with olanzapine and lower with haloperidol in a rat study [62]. Notwithstanding this finding, none of the PET studies have found correlations with current or past antipsychotic use [55–58]. Overall, whilst the present data cannot exclude an effect of antipsychotics

Table 4. Results from studies of SV2A PET in psychiatric illnesses.

Diagnosis	Reference	Comparison	Significant differences in SV2A PET measures (% difference, effect size)
Addictions	Angarita [68]	CoUD vs HC BP_{ND}	↓ ACC, ↓ vmPFC, ↓ mOFC
		CoUD vs HC V_T/fp	↓ ACC (d = 0.9), ↓ vmPFC (d = 0.83), ↓ mOFC (d = 0.75)
	D'Souza [69]	CaUD vs HC BP_{ND}	↓ Hip (−10.00%, d = 1.2)
	Hou [70]	IGD vs HC SUVR	↓ LN L, ↓ RO, ↓ ACC
Mood disorders	Holmes [64]	MDD/PTSD vs HC V_T	↓ dlPFC (−14.94%, d = 1.14), ↓ ACC (−15.76%, d = 1.3), ↓ Hip (−15.14%, d = 1.1), ↓ CBL (−14.17%, d = 1.54), ↓ FC (−15.28%, d = 1.18), ↓ OC (−14.08%, d = 1.12), ↓ PC (−14.66%, d = 1.03), ↓ Put (−13.67%, d = 1.18), ↓ TC (−14.38%, d = 1.21)
	Casteele [63]	Later life MDD vs HC SUVR	NS
	Holmes [66]	MDD/PTSD vs HC V_T	↓ dlPFC, ↓ ACC, ↓ Hip
		Low SV2A MDD/PTSD vs high SV2A post ketamine V_T	↑ dlPFC (8.70%, d = 1.1), ↑ ACC (10.40%, d = 1.2)
SZ	Onwordi [55]	SZ vs HC V_T	↓ FC (d = 0.8), ↓ ACC (d = 0.9), ↓ dlPFC (d = 0.9), ↓ TL (d = 0.9), ↓ OL (d = 0.8), ↓ PL (d = 0.7), ↓ Thal (d = 0.8), ↓ Amg (d = 0.7)
		SZ vs HC DVR	↓ FC (d = 1), ↓ ACC (d = 1), ↓ dlPFC (d = 1), ↓ TL (d = 1.1), ↓ OL (d = 0.9), ↓ PL (d = 0.9), ↓ Thal (d = 0.9)
	Onwordi [108]	SZ vs HC DVR	↓ ACC (d = 0.8)
		SZ vs HC V_T	↓ ACC (d = 0.9)
	Onwordi [56]	SZ vs HC V_T /fp	↓ TL (d = 0.7)
	Radhakrishnan [58]	SZ vs HC BP_{ND}	↓ FC (−10.00%, d = 1.01), ↓ ACC (−11.00%, d = 1.24), ↓ Hip (−15.00%, d = 1.29), ↓ OC (−14.00%, d = 1.34), ↓ PC (−10.00%, d = 0.03), ↓ TC (−11.00%, d = 1.23), ↓ Amg (−10.10%, d = 0.91), ↓ FG (−11.10%, d = 1.17), ↓ IC (−11.00%, d = 1.09), ↓ Pallidum (−11.60%, d = 0.98), ↓ Put (−8.10%, d = 0.83), ↓ Thal (−10.90%, d = 1), ↓ VS (−8.50%, d = 0.9)
		SZ vs HC V_T	↓ ACC (−8.10%, d = 0.87), ↓ Hip (−9.60%, d = 1.24), ↓ OC (−10.50%, d = 1.04), ↓ TC (−8.00%, d = 0.87)
	Yoon [57]	SZ vs HC BP_{ND}	↓ Amg L (−21.30%, d = 1.555), ↓ Pars triangularis R (−21.50%, d = 1.488), ↓ FP L (−21.60%, d = 1.485), ↓ Thal R (−17.00%, d = 1.454), ↓ Rost mFG R (−18.50%, d = 1.448), ↓ mOFC R (−18.40%, d = 1.446), ↓ lOFC R (−18.30%, d = 1.446), ↓ Hip R (−17.00%, d = 1.429), ↓ Put L (−16.90%, d = 1.425), ↓ Hip L (−18.20%, d = 1.421), ↓ HG R (−18.50%, d = 1.42), ↓ Rost mFG R (18.5%, d = 1.448), ↓ Hip R (17.00%, d = 1.429), ↓ Put L (16.9%, d = 1.425), ↓ Hip L (18.2%, d = 1.421), ↓ Heschl's R (18.50%, d = 1.42), ↓ sTG R (18.5%, d = 1.351), ↓ Caud mFG R (19.3%, d = 1.337), ↓ Put R (15.7%, d = 1.33)

If both PVC and non-PVC results were available, then only PVC were reported in the table. Nonsignificant findings are not reported, but full data can be accessed here GitHub.

↓ lower SV2A PET value in the region indicated, *ACC* anterior cingulate cortex, *Amg* amygdala, *BPnd* nondisplaceable binding potential, *CaUD* cannabis use disorder, *CBL* cerebellum, *CoUD* cocaine use disorder, *DVR* distribution volume ratio, *FG* frontal gyrus, *FP* frontal pole, *Hip* hippocampus, *i* inferior, *IC* insular cortex, *IGD* internet gaming disorder, *l* left, *LN* lenticular nucleus, *m* medial/middle, *MDD* major depressive disorder, *NR* not reported, *OC* occipital cortex, *OFC* orbitofrontal cortex, *OL* occipital lobe, *PC* parietal cortex, *PL* parietal lobe, *Put* putamen, *r* right, *RO* Rolandic operculum, *s* superior, *SUVR* standardised uptake value ratio, *SZ* schizophrenia, *TC* temporal cortex, *TG* temporal gyrus, *Thal* thalamus, *(vm/dlp)FC* (ventromedial/dorsolateral pre)frontal cortex, *Vt* volume of distribution.

on SV2A PET outcomes, it seems unlikely that antipsychotic treatment is having a major effect on them.

Major depression

Three PET studies have been performed investigating SV2A in major depressive disorder (MDD) (Table 4, Supplementary Table 3). These studies report diverging results, with Casteele et al. [63] showing no change in [^{11}C]UCB-J SUVR in later-life depression versus controls, while in a study including people with either MDD or posttraumatic stress disorder (PTSD), Holmes et al. [64] found lower [^{11}C]UCB-J V_T in the dorsolateral prefrontal cortex (dlPFC), hippocampus and anterior cingulate cortex (ACC) in patients with more severe depressive symptoms compared to controls. The use of different outcome measures may explain the divergence; SUVR studies are more sensitive to noise and inter-individual variability in tracer uptake than quantitative outcome measures using ABS, such as V_T (Box 1, Supplementary), and may be expected to require larger sample sizes to detect an effect [65]. In a separate study investigating treatment effects, Holmes et al. found that participants with low V_T showed significant increases in [^{11}C]UCB-J V_T following ketamine in the dlPFC and ACC (Table 4), which correlated with a greater reduction in depressive symptoms [66]. A caveat of this post-hoc analysis is that it could reflect regression to the mean. See the review on imaging findings in MDD in this issue of *Neuropsychopharmacology* for further discussion.

Holmes et al. also found that depressive symptoms negatively correlated with [^{11}C]UCB-J V_T in these three regions (Table 7), including in patients only with a PTSD diagnosis [64]. This was not found in a similar study by Asch et al. [67], who found no correlations between depressive symptomatology and [^{11}C]UCB-J V_T in subjects with obesity and various psychiatric diagnoses.

This study did, however, find significant correlations between anxiety ratings and [^{11}C]UCB-J V_T in prefrontal regions in all patients (Table 7). Unfortunately, no symptom correlations were explored in the later-life depression study [63]. These findings suggest that subclinical mood and anxiety symptoms may be associated with lower SV2A in the frontal cortex in patients across a range of different diagnoses, although current evidence is limited.

Substance use disorders and other addictions

Three studies have performed SV2A PET in addictions, using [^{11}C]UCB-J V_T/f_p in cocaine use disorder [68], [^{11}C]UCB-J BP_{ND} in cannabis use disorder [69], and [^{18}F]SynVesT-1 SUVR in gaming disorder [70] (Table 4, Supplementary Table 3). Each found lower tracer uptake in patients versus controls, but in mostly non-overlapping regions (Table 4). Only the ACC was implicated in more than one study, showing lower tracer uptake in cocaine use disorder and gaming disorder. Other regions showed lower tracer uptake in only one study: the PFC in cocaine use [68], the hippocampus in cannabis use [69], and the putamen in gaming disorder [70]. Relationships between tracer uptake in these regions with frequency of engagement with the addictive behaviour similarly varied, from significant negative correlations in gaming disorder, to no relationship in cannabis misuse, to significant positive correlations in cocaine misuse (Table 7). The latter finding is paradoxical, given the lower SV2A PET measures in the patient group. The authors suggest it is related to the formation of silent synapses in the brain during cocaine use, which has been observed in mice [71, 72]. They hypothesised that these synapses would be pruned after a period of abstinence, explaining the positive correlation with cocaine consumption. While a general pathophysiology underlying different addictions has been proposed [73], evidence from these three studies does not suggest there is a common pattern of synaptic terminal loss in specific brain regions based on the limited literature to date.

Alzheimer's dementia

16 studies have used SV2A PET imaging in AD; all finding lower SV2A PET measures in people with AD relative to controls, although several of these had overlapping samples (Supplementary Table 4). Findings consistent with lower SV2A levels in entorhinal cortex [74–77] and the hippocampus [28, 74, 76–83] (Table 5, Supplementary Table 4) were most widely reported. Studies also report changes in the amygdala [76, 77], the parahippocampus [76, 78], and the thalamus [74, 78, 81] (Table 5). In individuals with mild cognitive impairment (MCI) lower [^{11}C]-UCB-J SUVR was found in medial temporal lobe and hippocampus relative to controls [80]. When the same cohort was scanned after 2 years, a small decrease in [^{11}C]UCB-J SUVR compared to baseline was found in several cortical regions [79]. In contrast, a longitudinal study in AD found no significant differences in [^{11}C]UCB-J DVR versus baseline after 12–18 months [79, 81]. Taken with the findings in MCI, this could suggest that the early stages of AD are characterised by larger longitudinal reductions in SV2A levels than later stages of AD, but further longitudinal studies are needed to test this. O'Dell et al. [84] investigated relationships with amyloid-beta (Aβ), finding a negative correlation between [^{11}C]PiB DVR, a marker of Aβ deposition, and hippocampal [^{11}C]UCB-J DVR in a cohort of people with MCI AD ($r = -0.55$, $p = 0.04$), but not in an mild AD dementia cohort ($r = 0.05$, $p = 0.82$). These findings suggest that Aβ could be contributing to synaptic degeneration more at the MCI than the dementia stage, when Aβ levels tend to plateau [84].

Other primary tauopathies

Six cross-sectional studies have been published SV2A PET in non-AD tauopathies [85–90] (Table 5, Supplementary Table 4). Studies of progressive supranuclear palsy (PSP) and corticobasal degeneration (CBD) have consistently shown lower BP_{ND} with [^{11}C]UCB-J [85, 87, 90, 91], affecting most cortical and subcortical regions in CBD, and all regions reported in PSP (Table 5). Effect sizes for lower BP_{ND} versus controls in PSP were generally larger in the basal ganglia compared to CBD [85, 86]. A further two studies have reported findings specifically in behavioural variant fronto-temporal dementia (bvFTD) [88, 89]. Salmon et al. showed lower [^{18}F]UCB-H V_T in the parahippocampal gyrus only, which did not survive family-wise-error correction, while Malpetti et al. reported lower [^{11}C]UCB-J BP_{ND} in widespread cortical, but not subcortical, regions. The less extensive alterations seen in Salmon et al. could reflect the fact that their sample showed relatively milder impairments on the Mini Mental State Exam (MMSE) (patients = 25.4, controls = 29.1) than those in the study by Malpetti et al. (MMSE score: patients = 22.3, controls = 29.5). A further study investigated [^{11}C]UCB-J BP_{ND} in a sample that included patients with PSP, bvFTD or CBD [90]. They found globally lower BP_{ND} in the combined clinical group versus controls in cortical and subcortical regions in a voxel-wise analysis. Independent component analysis found more marked cortical SV2A changes in bvFTD than the other conditions. The component incorporating the medial parietal and frontal lobe showed lower BP_{ND} in CBD over PSP ($p = 0.024$), although no components showed lower BP_{ND} in PSP compared to the other clinical groups. These findings in total are broadly consistent with the clinical spectrum of tauopathies [92], with PSP showing greater pathology in subcortical nuclei, bvFTD more cortical pathology, and CBD showing similar involvement of both cortical and subcortical regions.

One study in CBD and PSP has investigated changes in synaptic measures over time. Holland et al. [91] found a significant overall decline in [^{11}C]UCB-J BP_{ND} over 1 year, particularly in the right caudate and left frontal cortex (Table 5). Using principal component analysis, the authors also showed that higher loading on a component incorporating the rate of reductions in frontal and cingulate cortical [^{11}C]UCB-J BP_{ND} were associated with faster progression of symptoms ($r = 0.47$, $p = 0.03$) and more rapid cognitive decline ($r = -0.62$, $p = 0.003$). Indeed, where this was reported, all cross-sectional studies described here also found significant negative correlations between BP_{ND} and symptom severity, including cognitive dysfunction. This was found in in striatal [90] regions and global GM [86] in PSP/CBD, and cortical regions in bvFTD [89] (Table 7). Overall, with the exception of one study in patients with milder illness, there is convergent evidence that tauopathy is associated with widespread reductions in SV2A PET measures, affecting expected regions based on the clinical syndrome and showing convincing relationships with symptoms.

α-Synucleinopathies

Four cross-sectional PET studies have been performed in Parkinson's disease (PD) [93–96] (Table 5 Supplementary Table 4). While all four found lower [^{11}C]UCB-J BP_{ND} [93], V_T [95] or SUVR [97, 98] in the patient group, there were no specific nuclei or cortical areas showing changes in all four studies (Table 5). The substantia nigra, a key nucleus in the pathophysiology of PD, showed significantly lower tracer uptake in three studies [93, 97, 98], while Wilson et al. [95] found changes in the dorsal raphe nuclei and the brainstem. Other brain regions implicated in each study varied, as did the clinical severity of each study's sample. Wilson et al. found fairly widespread lower V_T in cortical and subcortical regions (Table 5), surprisingly, in a patient group with the mildest symptom severity ratings of all the studies (mean Movement Disorder Society - Unified Parkinson's Disease Rating Scale III (MDS-UPDRS-III) score 20.1), and with no cognitive impairment. Given only two studies used the same outcome measure, it is difficult to assess whether different analysis methods may explain heterogeneity in the findings across regions or if it could relate to clinical differences, however it is notable that the two which used SUVR both found lower tracer uptake in the

Table 5. Results from studies of SV2A PET in neurodegenerative disorders.

Diagnosis	Reference	Comparison	Significant differences in SV2A PET measures (% difference, effect size, where reported)
AD/MCI	Bastin [78]	AD vs HC (V_T)	↓ Basal forebrain (−37.30%, d = 0.67), ↓ Hip (−30.90%, d = 1.24), ↓ OC (−17.20%, d = 0.65), ↓ PC (−17.60%, d = 0.69), ↓ pFC (−14.30%, d = 0.63), ↓ PPHG (15.60%, d = 0.71), ↓ TC (−14.90%, d = 0.65), ↓ Thal (−15.90%, d = 0.73)
	Chen [74]	AD vs HC (BP_{ND})	↓ EC, ↓ Hip (−44.00%)
		AD vs HC (V_T)	↓ EC, ↓ Hip (−28.00%), ↓ Pulvinar
	Chen [76]	AD vs HC (DVR)	↓ AG (8.70%, d = 0.91), ↓ Hip (24.80%, d = 1.93), ↓ PC (8.50%, d = 0.84), ↓ PHG (15.00%, d = 1.44), ↓ Pulvinar (18.30%, d = 1.55), ↓ TC (7.60%, d = 1.04), ↓ Thal (12.40%, d = 1.28)
		AD vs HC (DVR)	↓ Amg (17.10%, d = 1.25), ↓ EC (23.20%, d = 1.62)
	Lu [75]	AD vs HC (BP_{ND})	↓ EC, ↓ Hip
	Mecca [77]	AD vs HC (BP_{ND})	↓ Hip (20.00%)
	Tuncel [28]	AD vs HC (BP_{ND})	↓Hip (20.9%), ↓ MTL (17.3%), ↓ GM (16.9%)
	Vanderlinden [79]	aMCI Δ2 years (SUVR)	↓ CC (−6.80%), ↓ FC (−6.60%), ↓ Hip (−7.70%), ↓ Lateral TC (−6.30%), ↓ MsTC (−9.10%), ↓ OC (−6.00%), ↓ PC (−6.80%)
	Vanhaute [80]	MCI vs HC (SUVR)	↓ Hip (19.00%), ↓ TL (17.00%)
	Venkataraman [81]	AD vs MCI (DVR)	↓ CN (25.00%), ↓ Hip (24.00%), ↓ Thal (19.00%)
	Zhang [82]	AD vs HC (SUVR)	↓ FG L, ↓ Hip L, ↓ Hip R, ↓ IC L, ↓ IC R, ↓ iPG R, ↓ mFG, ↓ mFG L, ↓ PCG L, ↓ PoCG R, ↓ sFG L, ↓ sFG R
		AD vs MCI (SUVR)	↓ IC R, ↓ mFG L, ↓ mFG R
Other Primary Tauopathy	Holland [86]	CBD vs HC, PSP vs HC (BP_{ND})	↓ Amg (20%, 19%), ↓ CBL (18%, 21%), ↓ CG (15%, 19%), ↓ CN (17%, 21%), ↓ FL (12%, 16%), ↓ Hip (22%, 22%), ↓ Ins (19%, 21%), ↓ Medulla (40%, 55%), ↓ Midbrain (17%, 30%), ↓ NAcc (8%, 15%), ↓ OL (11%, 17%), ↓ PL (12%, 15%), ↓ Pons (19%, 24%), ↓ Put (14%, 18%), ↓ Thal (20%, 21%), ↓ TL (14%, 19%)
		PSP vs HC (BP_{ND})	↓ Pallidum (33.00%), ↓ SN (38.00%)
	Holland [85]	CBD vs HC, PSP vs HC (BP_{ND})	↓ Amg (d = 0.44 (0.12), 0.43 (0.1)), ↓ CBL (d = 0.40 (0.12), 0.41 (0.1)), ↓ CG (d = 0.37 (0.12), 0.52 (0.1)), ↓ CN (d = 0.48 (0.12), 0.65 (0.1)), ↓ FL (d = 0.31 (0.12), 0.44 (0.1)), ↓ Hip (d = 0.34 (0.12), 0.35 (0.1)), ↓ Ins (d = 0.43 (0.12), 0.50 (0.1)), ↓ Midbrain (d = 0.53 (0.12), 0.90 (0.1)), ↓ OL (d = 0.32 (0.12), 0.44 (0.1)), ↓ PL (d = 0.36 (0.12), 0.42 (0.1)), ↓ Put (d = 0.54 (0.12), 0.71 (0.1)), ↓ SN (d = 0.42 (0.12), 0.73 (0.1)), ↓ Thal (d = 0.72 (0.12), 0.59 (0.1)), ↓ TL (d = 0.34 (0.12), 0.44 (0.1))
		PSP vs HC (BP_{ND})	↓ Medulla (d = 0.30 (0.1)), ↓ NAcc (d = 0.62 (0.1)), ↓ Pallidum (d = 0.62 (0.1))
	Holland [91]	CBD vs HC (BP_{ND})	↓ CBL (mean Z-score −1.6), ↓ CN (mean Z-score −1.6), ↓ FL (mean Z-score −1.6), ↓ PL (mean Z-score −1.8), ↓ Put (mean Z-score −1.5), ↓ Thal (mean Z-score −1.8)
		PSP vs HC (BP_{ND})	↓ CC (mean Z-score −1.6), ↓ CN (mean Z-score −2.1), ↓ FL (mean Z-score −1.6), ↓ Midbrain (mean Z-score −1.6), ↓ Pallidum (mean Z-score −1.9), ↓ Thal (mean Z-score −1.6)
		ΔUCB-J PSP/CBD 1 y followup (BP_{ND})	↓ CN (−3.90%), ↓ Presubgenual FC (−3.50%)
	Whiteside [90]	PSP + CBS + bvFTD vs HC (BP_{ND})	↓ Widespread
	Malpetti [89]	bvFTD vs HC (BP_{ND})	↓ Amg L (24.00%, d = −1.48), ↓ Amg R (37.00%, d = −2.09), ↓ CC L (23.00%, d = −2.00), ↓ CC R (24.00%, d = −2.26), ↓ FC L (23.00%, d = −2.33), ↓ FC R (21.00%, d = −2.33), ↓ Hip L (26.00%, d = −1.14), ↓ Hip R (36.00%, d = −1.96), ↓ IC L (28.00%, d = −2.00), ↓ IC R (33.00%, d = −2.68), ↓ OC L (12.00%, d = −1.14), ↓ OC R (13.00%, d = −1.23), ↓ PC L (16.00%, d = −1.89), ↓ PC R (16.00%, d = −1.81), ↓ TC L (24.00%, d = −2.28), ↓ TC R (23.00%, d = −2.17), ↓ Thal L (26.00%, d = −1.80), ↓ Thal R (35.00%, d = −1.67)
α-synucleinopathy	Andersen [98]	DLB/PDD vs HC (SUVR)	↓ iPC, ↓ lateral OC, ↓ lateral OTC, ↓ M1S1, ↓ mFG, ↓ mOC, ↓ OFC, ↓ SN, ↓ sPL
		nPD vs HC (SUVR)	↓ SN

Table 5. continued

Diagnosis	Reference	Comparison	Significant differences in SV2A PET measures (% difference, effect size, where reported)
	Andersen [96]	DLB/PDD vs HC (SUVR)	↓ CBL (−26.00%), ↓ FC (−21.00%), ↓ IC (−46.00%), ↓ mTC (−20.00%), ↓ OC (−28.00%), ↓ PC (−25.00%), ↓ TC L (−21.00%), ↓ Thal (−22.00%)
	Delva [94]	PD vs HC (SUVR)	↓ SN (−14.40%)
	Delva [101]	PD vs HC (SUVR)	↓ SN (15.70%)
	Matuskey [93]	PD vs HC (BP_{ND})	↓ Locus coeruleus (17.00%), ↓ OFC (11.00%), ↓ PCC (15.00%), ↓ PHG (12.00%), ↓ Red nucleus (31.00%), ↓ SN (45.00%), ↓ vmPFC (11.00%)
	Nicastro [104]	LBD vs HC (BP_{ND})	↓ Cuneus, ↓ iFG, ↓ mFG, ↓ OCC, ↓ PCG, ↓ PL, ↓ sFG, ↓ sPC, ↓ sTC, ↓ TL
	Wilson [95]	PD vs HC (V_T)	↓ BS (9.40%, d = 0.81), ↓ CN (15.00%, d = 0.82), ↓ DRaphe (9.00%, d = 0.83), ↓ FC (10.30%, d = 0.86), ↓ Ins (7.90%, d = 0.77), ↓ OC (11.00%, d = 1), ↓ PC (11.00%, d = 0.88), ↓ Put (9.70%, d = 0.99), ↓ TC (9.00%, d = 0.92), ↓ Thal (11.60%, d = 0.74)
HD	Delva [97]	HD vs HC (SUVR)	↓ CBL (11% (± 9%)), ↓ CN (25% (± 14%)), ↓ FC (8% (± 8%)), ↓ OC (9% (± 8%)), ↓ Pallidum (24% (± 15%)), ↓ PC (9% (± 8%)), ↓ Put (28% (± 13%)), ↓ TC (9% (± 9%))
		mHD vs HC (SUVR)	↓ CBL (−14.00%), ↓ CN (−31.00%), ↓ FC (−11.00%), ↓ GM (−12.00%), ↓ Pallidum (−30.00%), ↓ PC (−11.00%), ↓ Put (−33.00%), ↓ TC (−12.00%)
		pmHD vs HC (SUVR)	↓ CN (−16.00%), ↓ Put (−19.00%)
	Delva [102]	ΔHD (Y0 vs Y2), ΔHC (Y0 vs Y2) (SUVR)	↓ CN (−4.5%, −0.8%), ↓ Put (−3.6%, −0.1%)
		ΔpmHD (Y0 vs Y2), ΔmHD (Y0 vs Y2) (SUVR)	↓ CN (−2.9%, −5.4%), ↓ Pallidum (−0.8%, −4.2%)
SCA	Chen [162]	Ataxic vs. HC (SUVR)	↓ CBL L (−11.43%), ↓ CBL R (−11.71%), ↓ CN L (−8.67%), ↓ CN R (−7.42%), ↓ Medulla (−8.33%), ↓ Midbrain (−7.61%), ↓ OC L (−4.95%), ↓ OC R (−4.94%), ↓ Pons (−8.03%), ↓ Put L (−3.96%), ↓ Put R (−3.55%), ↓ Vermis (−15.95%)
		Ataxic vs. pre-ataxic (SUVR)	↓ CBL L (−8.22%), ↓ CBL R (−7.69%), ↓ CN L (−7.33%), ↓ CN R (−5.60%), ↓ Medulla (−10.60%), ↓ Midbrain (−5.21%), ↓ OC L (−3.52%), ↓ OC R (−3.68%), ↓ Pons (−8.03%), ↓ Put L (−3.15%), ↓ Put R (−3.77%), ↓ Vermis (−10.75%)
		Pre-ataxic vs HC (SUVR)	↓ Vermis (not significant after PVC) (−5.83%)
TLE	Finnema [116]	Asymmetry in BP_{ND} in TLE vs HC	Amg (7% (± 6%), 3% (± 5%)), EC (3% (± 14%), 9% (± 6)), Fusiform (1% (± 6%), 8% (± 4)), Hip (17% (± 5%), 0% (± 4)), Ins (2% (± 4%), 10% (± 4)), ParaHip (0% (± 5%), 9% (± 6)), TC (1% (± 5%), 9% (± 4)), Thal (4% (± 6%), −1% (± 2))

If both PVC and non-PVC results were available, then only PVC were reported in the table. Nonsignificant findings are not reported, but full data can be accessed here GitHub.

↓ lower SV2A PET value in the region indicated, *AD* Alzheimer's dementia, *AG* angular gyrus, *Amg* amygdala, *BPnd* nondisplaceable binding potential, *BS* brainstem, *(bv)FTD* (behavioural variant) frontotemporal dementia, *CBD* corticobasal degeneration, *CBL* cerebellum, *CG* cingulate gyrus, *CN* caudate nucleus, *DRaphe* dorsal raphe, *DVR* distribution volume ratio, *EC* entorhinal cortex, *FG* frontal gyrus, *FL* frontal lobe, *GM* grey matter, *Hip* hippocampus, *i* inferior, *IC* insular cortex, *l* left, *m* medial/middle, *LBD* Lewy body dementia, *M1S1* primary sensorimotor cortex, *MCI* mild cognitive impairment, *MsTC* mesotemporal cortex, *NAcc* nucleus accumbens, *NR* not reported, *OC* occipital cortex, *OFC* orbitofrontal cortex, *OL* occipital lobe, *OTC* occipitotemporal cortex, *PC* parietal cortex, *PCC* posterior cingulate cortex, *PCG* posterior cingulate gyrus, *PD* Parkinson's disease, *(pm)HD* (premanifest) Huntington's disease, *PoCG* postcentral gyrus, *PL* parietal lobe, *PHG* parahippocampal gyrus, *PSP* progressive supranuclear palsy, *Put* putamen, *PVC* partial volume correction, *r* right, *s* superior, *SCA* spinocerebellar ataxia, *SN* substantia nigra, *SUVR* standardised uptake value ratio, *Thal* thalamus, *TLE* temporal lobe epilepsy, *(vm/dlp)FC* (ventromedial/dorsolateral pre)frontal cortex, *Vt* volume of distribution.

substantia nigra only, despite including patients with relatively severe symptoms (MDS-UPDRS-III) score 26.6 [96] and 41.5 [94] respectively).

Two longitudinal studies found no significant change in SV2A PET measures over 10–24 months, despite progression in MDS-UPDRS-III ratings from 24.3 to 27.6 [97] and 23.3 to 31.3 [95] respectively, suggesting that changes detected with SV2A PET are not related to motor progression; only one study [97] reported correlations, but these were nonsignificant. In contrast, uptake of the dopamine transporter (DAT) tracer [18 F]FE-PE2I showed longitudinal decline, which correlated with increasing clinical scores in the putamen ($r = -0.53$) and dorsal striatum ($r = -0.51$) contralateral to the least affected body side at follow-up.

SV2A imaging in PD does therefore show evidence for lower tracer uptake in expected mesencephalic regions, however the anatomical extent and severity of synaptic protein loss shows little relationship with motor symptoms, except in participants with mild [95] or subclinical [99] disease. Taken with dopaminergic imaging findings that do show relationships with motor symptoms [97], this indicates that SV2A PET is unlikely to provide much

Table 6. Results from correlations with other imaging measures.

Imaging Modality	Sample	Regional SV2A	Finding	Study
GMV	**CoUD**	ACC V_T/fp	$r = -0.16$ (NS)	Angarita [68]
		VS V_T /fp	$r = 0.19$ (NS)	
		lOFC V_T /fp	$r = -0.01$ (NS)	
		mOFC V_T /fp	$r = 0.37$ (NS)	
		vmPFC V_T /fp	$r = -0.06$ (NS)	
	MDD	Hip NR	NR (NS)	Casteele [63]
		TC NR	NR (NS)	
		pFC NR	NR (NS)	
	AD	Fusiform L V_T	$r = 0.45$	Moallemian [83]
		Hip L V_T	$r = 0.47$	
		Hip R V_T	$r = 0.19$ (NS)	
		PHG R V_T	$r = 0.22$ (NS)	
		TC L V_T	$r = -0.01$(NS)	
	LBD	Global BP_{ND}	NR (NS)	Nicastro [104]
	SZ	ACC V_T	$r = 0.19$ (NS)	Onwordi [55]
		FC V_T	$r = 0.20$ (NS)	
		Hip V_T	$r = 0.21$ (NS)	
	SZ	ACC BP_{ND}	$r = -0.14$ (NS)	Radhakrishnan [58]
		FC BP_{ND}	$r = 0.-0.01$(NS)	
		OC BP_{ND}	$r = 0.14$ (NS)	
		PC BP_{ND}	$r = 0.49$ (NS)	
		TC BP_{ND}	$r = -0.22$ (NS)	
		mTC V_T	$r = 0.70$	Salmon [88]
NDI	**AD + HC**	FL DVR	$R^2 = 0.17$	Venkataraman [81]
		PL DVR	$R^2 = 0.33$	
ODI	**PSP, CBS**	Widespread	NR	Mak [87]
	HC	Widespread	NR	
	AD + HC	PL DVR	$R^2 = 0.15$	Venkataraman [81]
		CN DVR	$R^2 = 0.20$	
	PSP, CBS, bvFTD	Global BP_{ND}	$\beta = 0.54$	Whiteside [90]
	HC	Global BP_{ND}	$\beta = 0.39$	
MRS (ACC Glu/Cr)	**SZ**	ACC DVR	$r = 0.32$ (NS)	Onwordi [108]
		Hip DVR	$r = 0.30$ (NS)	
FC	**HC**	Striatum V_T	$r = 0.44$	Fang [52]
		mPFC V_T	$r = 0.64$	
		mPFC V_T	$r = 0.36$	
		mPFC V_T	$r = 0.35$	
		Striatum V_T	$r = 0.34$	
	PSP, CBD, bvFTD	Striatal ICA BP_{ND} loading	$\beta = 0.4$	Whiteside [90]
		Medial PL/FL ICA BP_{ND} loading	$\beta = 0.29$	
		Left frontoparietal ICA BP_{ND} loading	$\beta = 0.27$	
		Posterior cingulate ICA BP_{ND} loading	$\beta = 0.43$	
		Left lateral frontal lobe ICA BP_{ND} loading	$\beta = 0.40$	
FC (lMFG)	**AD + MCI**	mFG L SUVR	$r = 0.73$	Zhang [82]
		mFG R SUVR	$r = 0.61$	
FC (lMFG-lIFG)	**AD + MCI + HC**	mFG L SUVR	$r = 0.67$	
		mFG R SUVR	$r = 0.61$	
FC (dlPFC-PCC)	**MDD**	dlPFC V_T	$r = -0.6$	Holmes [64]
[^{18}F]flortaucipir BP_{ND}	**AD**	Multiple ROI BP_{ND}	$r = -0.47$	Coomans [111]
[^{18}F]flortaucipir SUVR (EC)	**AD + HC**	Hip DVR	$r = -0.61$	Mecca [103]

Table 6. continued

Imaging Modality	Sample	Regional SV2A	Finding	Study
[^{18}F]AV-1451 BP_{ND} (global)	**PSP, CBS**	Global BP_{ND}	$\beta = 0.4$, $t = 3.6$,	Holland [85]
[^{18}F]-MK-6240 SUVR (MTL)	**MCI**	MTL SUVR	$r = -0.76$	Vanhaute [80]
[^{18}F]-MK-6240 SUVR	**MCI**	TC, TPC, OC SUV	Negative correlations (voxelwise)	Vanderlinden [79]
[^{18}F]FDG PET	**AD**	Hip DVR	$R^2 = 0.86$	Chen [76]
		Precuneus DVR	$R^2 = 0.59$	
	TLE	Hip BPnd	$R^2 = 0.38$	Finnema [116]
[^{18}F]FDG PET (CN)	**HD**	Global SUVR	$R^2 = 0.50$	Delva [97]
[^{18}F]FDG PET (putamen)		Global SUVR	$R^2 = 0.55$	
[^{11}C]PiB DVR (global)	**AD**	IPC DVR	$r = 0.03$	O'Dell [84]

If both PVC and non-PVC results were available, then only PVC were reported in the table. Nonsignificant findings are not reported, except where relevant to the main text, but full data can be accessed here GitHub.

AD Alzheimer's dementia, *AG* angular gyrus, *Amg* amygdala, *BPnd* nondisplaceable binding potential, *(bv)FTD* (behavioural variant) frontotemporal dementia, *CBD* corticobasal degeneration, *CBL* cerebellum, *CG* cingulate gyrus, *CN* caudate nucleus, *DRaphe* orsal raphe, *DVR* distribution volume ratio, *EC* entorhinal cortex, *FG* frontal gyrus, *FISO* fraction of Gaussian isotropic diffusion, *FL* frontal lobe, *GM(V)* grey matter (volume), *HC* healthy control, *Hip* hippocampus, *i* inferior, *IC* insular cortex, *K1* delivery rate constant, *Ki* inhibition constant, *l* lateral, *L* left, *m* medial/middle, *LBD* Lewy body dementia, *MCI* mild cognitive impairment, *MDD* major depressive disorder, *MTL* medial temporal lobe, *NDI* neurite density index, *NR* not reported, *OC* occipital cortex, *ODI* orientation dispersion index, *OL* occipital lobe, *PC* parietal cortex, *PCC* posterior cingulate cortex, *PCG* posterior cingulate gyrus, *PD* Parkinson's disease, *(pm)HD* (premanifest) Huntington's disease, *PL* parietal lobe, *PHG* parahippocampal gyrus, *PSP* progressive supranuclear palsy, *PTSD* posttraumatic stress disorder, *R1* ROI delivery rate constant (K1) normalised to cerebellar K1, *r* right, *ROI* region of interest, *s* superior, *SN* substantia nigra, *SUVR* standardised uptake value ratio, *SV2A* synaptic vesicle glycoprotein 2A, *SZ* schizophrenia, *Thal* thalamus, *TLE* temporal lobe epilepsy, *TPC* temporoparietal cortex, *(vm/dlp)FC* (ventromedial/dorsolateral pre)frontal cortex, *VOI* volume of interest, *Vt* volume of distribution.

clinical value in evaluating motor symptoms of PD. Nevertheless, synaptic alterations may underlie cognitive impairments in PD [100]. Significant negative correlations between tracer uptake and cognitive performance were found in patients with Lewy body dementia (LBD) and PD dementia by Andersen et al., but only Matuskey et al. analysed relationships between BP_{ND} and cognitive function in people with PD without dementia. They found no significant correlations between cognitive scores and tracer uptake, but their analysis was restricted to SV2A measures in subcortical areas and motor cortex. It would be useful for future studies to investigate relationships in cortical regions which may be more closely implicated to cognitive impairments.

Huntington's disease

Two SV2A PET studies have been conducted in Huntington's disease (HD); one cross-sectional [101] and the second its longitudinal extension [102] (Table 5, Supplementary Table 4). Delva et al. [101] measured [^{11}C]UCB-J SUVR in 18 patients with HD, 7 of whom had premanifest disease (i.e., not showing motor signs), compared to 15 controls. [^{11}C]UCB-J uptake was significantly lower in total GM in the manifest group versus controls, as well as in widespread cortical, cerebellar and subcortical regions (Table 5). Voxelwise analysis showed the most marked differences were in the bilateral striatum and thalamus. The premanifest group showed lower [^{11}C]UCB-J SUVR versus controls in the putamen and caudate nucleus only (Table 5). [^{11}C]UCB-J SUVR-1 in the caudate was significantly correlated with more severe motor symptoms (Table 7), indicating that the motor symptoms of HD are related to synaptic changes in striatal regions. Repeated measures after a 2-year interval found that the premanifest group had progressed to show similar regional reductions in the SV2A marker as the manifest group when compared to controls. However, change in symptoms in the whole cohort did not correlate with changes in SUVR. Notwithstanding this, the HD findings suggest lower SV2A is localised to striatal regions before motor symptom onset in HD, and spreads to include much of the brain's GM in manifest disease.

Relationships between SV2A PET measures and magnetic resonance imaging

The relationship between SV2A PET measures and GM volume (GMV) measured using MRI was reported in nine studies [55, 58, 63, 68, 77, 83, 88, 103, 104]. While studies frequently found GM atrophy across disorders, only two found positive correlations between GMV and SV2A PET tracer uptake in patients [83, 88], with five studies finding no relationships [55, 58, 63, 68, 104] (Table 6). In tauopathies, illnesses strongly associated with brain atrophy [105], lower GMV was anatomically less extensive than lower SV2A tracer uptake [77, 90] and showed smaller effect sizes in group comparisons [87], suggesting that SV2A changes may precede detectable GM atrophy in neurodegeneration. One study also reported that GMV showed weaker correlations with cognitive dysfunction than did SV2A tracer uptake [103]. This could suggest that the GMV signal is less closely related to the pathophysiological process underlying symptoms than SV2A measures [106].

Neurite orientation dispersion and density imaging (NODDI) can provide measures of both the density and angular variation of neurites, with the signal dependent on factors such as dendritic arborisation [107]. Orientation dispersion imaging (ODI) has been measured in three tauopathy studies which also reported SV2A PET measures [81, 87, 90]. All three showed positive correlations with SV2A tracer uptake, which were widespread across the brain in two [87, 90] but limited to the parietal lobe and caudate in the third study [81], which also showed positive correlations between BP_{ND} and neurite density (Table 6). Two of these studies [81, 90] additionally detected positive correlations in healthy controls. NODDI is still a novel imaging measure, however, and further work is needed to understand how NODDI findings relate to synaptic loss, and SV2A imaging.

The use of multimodal imaging can also provide information on the loss of specific synapses. Onwordi et al.'s study in schizophrenia [108] investigated correlations between SV2A and regional glutamate concentrations as measured by proton magnetic resonance spectroscopy (MRS). There was a significant

positive correlation between SV2A measures and glutamate in the hippocampus and ACC of healthy participants, suggesting that a large proportion of the SV2A PET signal is related to glutamatergic terminals. Interestingly, this relationship was lost in people with schizophrenia. Putatively this could be explained by the depletion of glutamatergic terminals in the condition, which would be anticipated to weaken the normal correlation between SV2A levels and glutamate levels. However, this interpretation remains speculative [109].

Finally, four studies [52, 64, 82, 90] investigated relationships between SV2A PET and functional connectivity in the frontal lobe, as measured by BOLD MRI (Table 6). Fang et al.'s study in healthy controls [52] found significant positive correlations between [^{11}C]UCB-J V_T in both the medial PFC and striatum and connectivity of the anterior default mode network, measured with fractional amplitude of low-frequency fluctuations, a resting-state MRI measure indexing network connectivity. Whiteside et al.'s analysis [90] combining people with tauopathy and healthy volunteers found significant positive associations between [^{11}C]UCB-J BP_{ND} and functional connectivity. Positive correlations in both healthy controls and patients were also found in an AD study [82], where tracer uptake in the middle frontal gyrus correlated with that region's functional connectivity with the inferior and superior frontal gyri (Table 6). In Holmes et al.'s MDD study [64], dlPFC [^{11}C]UCB-J V_T was negatively correlated with dlPFC-posterior cingulate functional connectivity in the patient group. The authors suggest that this reflects lower SV2A levels underlying weaker switching between the central executive and default mode networks. Overall, the fMRI findings suggest that SV2A levels in some regions influence the connectivity of neural networks, consistent with a central role for synapses in brain network function.

Relationships between SV2A and other PET measures. Five studies [79, 80, 85, 110, 111] compared SV2A and tau accumulation, measured with the PET tracers [^{18}F]flortaucipir or [^{18}F]AV-1451. SV2A tracer uptake and tau accumulation were negatively correlated in AD [110, 111], as well as in MCI [80] (Table 6), but positively correlated in PSP/CBD [85]. However, the spatial pattern of tau accumulation was more widespread than the regions showing lower [^{11}C]UCB-J BP_{ND} or SUVR [80, 111]. At 2 year follow up, tau accumulation and reductions in SV2A tracer uptake in MCI continued to follow this spatial pattern, with tau accumulation remaining more widespread, preceding later changes in SV2A measures [79]. Two studies, in AD [84] and PSP/CBD [90] respectively, reported that at the individual level, lower tau correlates with higher SV2A, but this relationship becomes negative with higher cortical tau, explaining the positive correlation detected by Holland et al. [85]. This may reflect a degree of compensatory upregulation of synapses early in the disorder, which has been reported in mouse models of mutant tau overexpression [112]. These studies are therefore consistent with the theory suggesting that tau accumulation precedes and underlies synaptic pathology in tauopathies [112–115]. This could be tested by determining whether tau PET measures predict the subsequent SV2A reductions.

Three studies have investigated correlations between between FDG and SV2A PET measures, finding significant positive correlations between the measures in AD [76], HD [101] and temporal lobe epilepsy [116] (Table 6). This is expected, considering synapses are responsible for 43–55% of brain adenosine triphosphate (ATP) use [117, 118]. However, interestingly, there is evidence for a greater spatial extent of FDG than SV2A PET alterations, indicating FDG may capture metabolic signs of synaptic impairment before overt loss of synaptic terminals [119]. However, it is important to note FDG changes could also reflect degeneration of the axons, glia and cell bodies, which make up the remaining half of brain ATP use [117].

DISCUSSION

Comparison of findings across disorders

SV2A PET studies have shown lower tracer brain uptake in every illness studied to date, although the specific regions involved and the effect size of findings often vary between studies of the same disorders, and there are some inconsistencies. Several factors, including analysis methods, study power, differences in stage or severity of disorder or other sources of heterogeneity, could contribute to inconsistencies between studies. We recommend data sharing as one strategy to address some of these issues, as this would permit the same analysis to be used for all data, boost power, and potentially enable clinical sources of heterogeneity to be investigated. Interestingly, the hippocampus and PFC were implicated in most illnesses studied (Tables 4, 5), with the exception of primary motor disorders. This is consistent with the hippocampus and PFC being regions implicated in a variety of affective, intellectual and motivational processes which are central to illnesses with behavioural and cognitive symptoms [120]; and is consistent with evidence that hippocampal-prefrontal pathways consistently show dysfunction in electrophysiological and neuroimaging studies across multiple psychiatric illnesses [120, 121]. Generalised cortical changes were characteristic of neurodegenerative illnesses associated with dementia, in particular tauopathies, HD, PD dementia and LBD. Subcortical changes were seen in all illnesses with motor symptoms, such as spinocerebellar ataxia, HD, PSP and PD, but also in schizophrenia and MDD, which could reflect the role of these regions in salience and affective states [122]. It should be noted, however, that while disorders may show involvement of the same brain regions, the mechanisms behind altered SV2A may differ between illnesses, and could preferentially affect synapses in specific cortical layers, as may be the case in schizophrenia [123], or of a certain neurotransmitter class.

An important consideration is that SV2A alterations in the disorders we have reviewed may not be causal. They could be the secondary consequences of other brain changes and/or confounders associated with the disorder. For example, neuropsychiatric disorders are often associated with social isolation. Indeed, reduced synaptic density secondary to isolation and reduced environmental richness has been detected in animal models [124], which has measurable effects on cognition [125]. Notwithstanding these considerations, findings that SV2A PET measures in cortical regions are related to functional connectivity measures across the brain highlights that SV2A alterations in specific cortical regions could have widespread effects, and potentially lead to mood [126] and anxiety [127] symptoms, negative symptoms [128], and cognitive impairments [129]. This could account for observations that these symptoms and impairments are seen in many neurological and psychiatric disorders. To date, longitudinal studies have shown decreases in SV2A PET measures and worsening of symptoms in neurodegenerative illnesses, supporting a causal role for synaptic changes in these disorders, but there have not been longitudinal studies in psychiatric disorders. These would be of high value to help determine causal relationships between synaptic alterations and psychiatric outcomes.

Relationship between SV2A PET measures and cognitive function

24 studies have correlated SV2A PET indices with cognitive measures, with twenty showing significant correlations (Table 7); four did not [93, 97, 98, 111]. In all studies reporting significant findings, lower SV2A PET measures in cortical regions correlated with poorer cognitive function. These covered a range of neuropsychiatric conditions, including mood disorders [67, 130], schizophrenia [57, 58], addictions [69, 70], AD [74, 77–82, 103], amyloid-negative tauopathies [86, 89–91], LBD [98] and HD [101]; this HD study was the only one showing significant correlations between cognition and subcortical tracer uptake, but these did not survive correction for multiple comparisons.

Table 7. Results from correlations of regional or global SV2A measures with symptoms and cognitive measures across psychiatric and neurodegenerative diagnoses.

Symptom/ cognitive domain	Diagnosis	Measure	Region	Finding	Study
Attention	**SZ**	Detection Test	OC BP_{ND}	$r = -0.66$	Radhakrishnan [58]
Executive function	**AD**	TMT-B, SCWT	AD-affected ROI DVR	$R^2 = 0.30$	Mecca [110]
	IGD	SSRT	ACC SUVR	$r = -0.573$	Hou [70]
			RO R	$r = -0.527$	
	LBD	MoCA executive function domain	mFG SUVR	$R^2 = 0.307$	Andersen [98]
	bvFTD	IFS	CC BP_{ND}	$r = 0.620$	Malpetti [89]
			FL BP_{ND}	$r = 0.754$	
			PL BP_{ND}	$r = 0.025$	
			voxelwise BP_{ND}	$r \geq 0.8$	
Global cognition	**AD**	CDR-SB	Hip BP_{ND}	$r = -0.61$	Chen [74]
			Hip DVRcb	$r = -0.62$	Mecca [77]
		MMSE	Hip DVR	$r = 0.77$	Vanhaute [80]
			Hip V_T	$r = 0.57$	Bastin [78]
			TL V_T	$r = 0.41$	
			pFC V_T	$r = 0.40$	
		Global Cognition	AD-affected ROI DVR	$R^2 = 0.33$	Mecca [110]
	AD + MCI	MMSE	Hip R SUVR	$r = 0.309$	Zhang [82]
			mFG-sFG R connectivity	$r = 0.289$	
	AD + MCI + HC	MMSE	IC R SUVR	$r = 0.213$	
			mFG L SUVR	$r = 0.124$	
			mFG R SUVR	$r = 0.278$	
			mFG-sFG R connectivity	$r = 0.231$	
	PSP, CBS	ACE R	global BP_{ND}	$r = 0.52$	Holland [86]
		Rate of change in ACE R	Δglobal BP_{ND}	$r = -0.62$	Holland [91]
	SZ	BACS	HG R	$R^2 = 0.339$	Yoon [57]
			mFG R	$R^2 = 0.286$	
			sTG R	$R^2 = 0.321$	
	MCI + HC	MMSE	mTL SUVR	$r = 0.47$	Vanderlinden [79]
	bvFTD	ACE R	CC BP_{ND}	$r = 0.700$	Malpetti [89]
			FL BP_{ND}	$r = 0.791$	
			PL BP_{ND}	$r = 0.591$	
			voxelwise BP_{ND}	$r \geq 0.8$	
	PSP, CBS, bvFTD	ACE-R	Medial PL/FL ICA BP_{ND} loading	$\beta = 0.44$	Whiteside [90]
			Frontoparietal ICA BP_{ND} loading	$\beta = 0.49$	
			ACC/IC ICA BP_{ND} loading	$\beta = 0.64$	
			Lateral FL ICA BP_{ND} loading	$\beta = 0.47$	
Language	**AD**	BNT	AD-affected ROI DVR	$R^2 = 0.23$	Mecca [110]
		Picture naming & semantic fluency	Hip DVR	$R^2 = 0.68$	Venkataraman [81]
			PL DVR	$R^2 = 0.39$	Venkataraman [81]
Memory	**AD**	episodic memory	Hip BP_{ND}	$r = 0.56$	Chen [74]
Processing speed	**AD**	TMT-A, DSS	AD-affected ROI DVR	$R^2 = 0.28$	Mecca [110]
Social cogniton	**SZ**	MATRICS SEC	PCC BP_{ND}	$r = 0.74$	Radhakrishnan [58]
		MCCB	FC BP_{ND}	$r = 0.64$	

Table 7. continued

Symptom/ cognitive domain	Diagnosis	Measure	Region	Finding	Study
Verbal memory	**AD**	RAVLT	Hip DVR	$r = 0.60$	Vanhaute [80]
		RAVLT DR	Hip DVR	$r = 0.70$	
		RAVLT DR	AD-affected ROI DVR	$R^2 = 0.24$	Mecca [110]
	AD + MCI	AVLT	IC R SUVR	$r = 0.279$	Zhang [82]
			mFG L SUVR	$r = 0.259$	
			mFG R SUVR	$r = 0.282$	
		BNT	Hip L SUVR	$r = 0.390$	
			Hip R SUVR	$r = 0.460$	
			IC R SUVR	$r = 0.281$	
			mFG L SUVR	$r = 0.257$	
			mFG R SUVR	$r = 0.262$	
		RAVLT	Hip L SUVR	$r = 0.467$	
			Hip R SUVR	$r = 0.533$	
	CaUD	RAVLT	Hip BPND	$\Phi = 0.67$	D'Souza [69]
	LBD	MoCA (language domain)	OTC SUVR	$R^2 = 0.060$	Andersen [98]
	MDD/PTSD	ISL	ACC V_T	$r = 0.41$	Holmes [64]
	MCI + HC	AVF	mTL SUVR	$r = 0.42$	Vanderlinden [79]
		RAVLT	mTL SUVR	$r = 0.53$	
			mTL SUVR	$r = 0.47$	
Visual attention	**NWPsy + OWPsy**	Identification Test (response time)	CBL V_T	$r = -0.501$	Asch [67]
			Hip V_T	$r = -0.422$	
			OFC V_T	$r = -0.420$	
			dlPFC V_T	$r = -0.439$	
			vmPFC V_T	$r = -0.444$	
Visuospatial	**AD**	DMS48	PHG V_T	$r = 0.46$	Bastin [78]
		WAIS-III block design, WAIS-III picture completion, ROCF	AD-affected ROI DVR	$R^2 = 0.23$	Mecca [110]
	AD + MCI	STT	Hip L SUVR	$r = -0.348$	Zhang [82]
	LBD	MoCA (visuospatial domain)	OC SUVR	$R^2 = 0.137$	Andersen [98]
			mOC SUVR	$R^2 = 0.155$	
CBD symptoms	**PSP, CBS**	CBD Rating Scale	Global BP_{ND}	$r = -0.72$	Holland [86]
PSP symptoms	**PSP, CBS**	PSP Rating Scale	Global BP_{ND}	$r = -0.61$	Holland [86]
	PSP, CBS, bvFTD		Striatal ICA BP_{ND} loading	$\beta = -0.5$	Whiteside [90]
	PSP, CBS	Rate of change in PSP rating scale	Δglobal BP_{ND}	$r = 0.47$	Holland [91]
Anosognosia	**AD**	AQ-D	Hip V_T	$r = -0.75$	Bastin [78]
			PCC V_T	$r = -0.43$	
		MARS	Hip V_T	$r = -0.75$	
			PCC V_T	$r = -0.48$	
			PHG V_T	$r = -0.48$	
			Thal V_T	$r = -0.48$	
			pFC V_T	$r = -0.47$	
	bvFTD	AQ-D	CN R V_T	$r = -0.89$	Salmon [88]
			FP R V_T	$r = -0.87$	
Anxiety symptoms	**NWPsy + OWPsy**	PSWQ	dlPFC V_T	$r = -0.463$	Asch [67]
Internet gaming	**IGD**	IGD89-SF	Putamen L SUVR	$r = -0.48$	Hou [70]
			Putamen R SUVR	$r = -0.48$	
		Daily gaming	Putamen L SUVR	$r = -0.57$	
		Daily gaming	Putamen R SUVR	$r = -0.59$	

Table 7. continued

Symptom/ cognitive domain	Diagnosis	Measure	Region	Finding	Study
Cocaine use	**CoUD**	abstinence	ACC V_T /fp	$i = -0.66$	Angarita [68]
			VS V_T /fp	$r = -0.56$	
			dmPFC V_T /fp	$r = -0.58$	
			vmPFC V_T /fp	$r = -0.61$	
		frequency	ACC V_T /fp	$r = 0.59$	
			OFC V_T /fp	$r = 0.56$	
			dmPFC V_T /fp	$r = 0.57$	
			vmPFC V_T /fp	$r = 0.58$	
Depressive symptoms	**MDD/PTSD**	HAMD-17	ACC V_T	$r = -0.63$	Holmes [64]
			Hip V_T	$r = -0.49$	
			dlPFC V_T	$r = -0.63$	
Parkinson's symptoms	**PD**	MDS-UPDRS total	BS V_T	$r = -0.63$	Wilson [95]
		MDS-UPDRS-III	BS V_T	$r = -0.66$	
			CBL SUVR	$\beta = -1.64$	Van Cauwenberge [99]
			CN SUVR	$\beta = -1.06$	
			OC SUVR	$\beta = -0.86$	
			PC SUVR	$\beta = -0.91$	
			SN SUVR	$\beta = -3.08$	
			TC SUVR	$\beta = -0.82$	
			Thal SUVR	$\beta = -2.30$	
Huntington's symptoms	**HD**	UHDRS motor score	Putamen SUVR	$R^2 = 0.67$	Delva[101]
Psychosis symptoms	**SZ**	PANSS positive	FC BP_{ND}	$r = -0.57$	Radhakrishnan [58]
		PANSS total	Hip V_T	$r = -0.48$	Onwordi [56]
		PANSS positive	mFG R BP_{ND}	$r = -0.668$	Yoon [57]

If both PVC and non-PVC results were available, then only PVC were reported in the table. Nonsignificant findings are not reported, but full data can be accessed here GitHub.

ACC anterior cingulate cortex, *ACE-R* Addenbrooke's Cognitive Examination Revised, *AD* Alzheimer's dementia, *AQ-D* Anosognosia Questionnaire – Dementia, *AVF* animal verbal fluency, *BACS* Brief Assessment of Cognition in Schizophrenia, *BNT* Boston Naming Task, *BPAD* bipolar affective disorder, *BPnd* nondisplaceable binding potential, *BS* brainstem, *(bv)FTD* (behavioural variant) frontotemporal dementia, *CaUD* cannabis use disorder, *CBD* corticobasal degeneration, *CBL* cerebellum, *CDR-SB* Clinical Dementia Scale Sum of Boxes, *CN* caudate nucleus, *CoUD* cocaine use disorder, *DMS* delayed match to sample, *DSS* digit/symbol substitution, *DVR* distribution volume ratio, *EC* entorhinal cortex, *FG* frontal gyrus, *FL* frontal lobe, *fp* plasma free fraction, *FP* frontal pole, *GAD* generalised anxiety disorder, *GM* grey matter, *HAMD-17* Hamilton Rating Scale for Depression, *HC* healthy control, *HG* Heschl's gyrus, *Hip* hippocampus, *i* inferior, *IC* insular cortex, *ICA* independent component analysis, *IFS* INECO Frontal Screening, *IGD* internet gaming disorder, *IGDS9-SF* Nine-Item Internet Gaming Disorder Scale, *ISL* International Shopping List, *l* left, *m* medial/middle, *LBD* Lewy body dementia, *MARS* Memory Awareness Rating Scale, *MCCB* MATRICS Consensus Cognitive Battery, *MCI* mild cognitive impairment, *MDD* major depressive disorder, *MDS-UPDRS* Movement Disorder Society Unified Parkinson's Disease Rating Scale, *MMSE* mini mental state examination, *MoCA* Montreal Cognitive Assessment, *NWPsy* normal weight with psychiatric diagnosis (MDD, PTSD, BPAD, GAD), *OC* occipital cortex, *OFC* orbitofrontal cortex, *OTC* occipitotemporal cortex, *OWPsy* overweight with psychiatric diagnosis (MDD, PTSD, BPAD, GAD), *PANSS* positive and negative symptom scale, *PC* parietal cortex, *PCC* posterior cingulate cortex, *PD* Parkinson's disease, *(pm)HD* (premanifest) Huntington's disease, *(dl/dm/vm)PFC* (dorsolateral/dorsomedial/ventromedial) prefrontal cortex, *PHG* parahippocampal gyrus, *PL* parietal lobe, *PSP* progressive supranuclear palsy, *PSWQ* Penn State Worry Questionnaire, *PTSD* posttraumatic stress disorder, *Put* putamen, *r* right, *RAVLT(DR)* Rey Audioverbal Learning Test (Delayed Recall), *RO* Rolandic operculum, *ROCF* Rey-Osterrieth Complex Figure, *ROI* region of interest, *s* superior, *SCWT* Stroop colour/word test, *SDMT* Symbol Digit Modalities Test, *SN* substantia nigra, *SSRT* stop signal reaction time, *STT* Shape Trail Test, *SUVR* standardised uptake value ratio, *SZ* schizophrenia, *Thal* thalamus, *TMT* Trailmaking Test, *UHDRS* Unified Huntington's Disease Rating Scale, *(vm/dlp)FC* (ventromedial/dorsolateral pre)frontal cortex, *VS* ventral striatum, *Vt* volume of distribution, *WAIS* Weschler Adult Intelligence Scale.

Significant correlations are reported between SV2A PET measures for whole GM and several cognitive domains, including language, executive functioning, processing speed, verbal and visuospatial memory, and global cognition (Table 7). However, studies have also investigated relationship between SV2A measures in specific regions and cognitive measures; including the PFC, where lower tracer uptake was associated with deficits in executive and social functioning, processing speed, and measures of global cognitive function, and the temporal cortex, where reduced tracer uptake was associated with deficits in audioverbal memory, episodic memory, and measures of global cognition (Table 7). Whilst this might be expected for global cognitive measures, it raises the question of whether it is global or regional SV2A levels that matters most for specific aspects of cognitive performance. Table 7 shows that correlations between audioverbal learning scores and temporal and hippocampal SV2A tracer measures were stronger ($r = 0.42$–0.7) in absolute terms than correlations with frontal, insular, and ACC uptake ($r = 0.26$–0.48; Table 7), consistent with evidence that temporal regions are most strongly implicated in audioverbal learning processes [131]. Similarly, significant correlations involving executive and inhibitory functions were largely limited to the frontal lobe and ACC (Table 7). Thus, the evidence to date indicates that regional SV2A is most strongly related to region-specific aspects of cognitive performance.

Limitations of SV2A PET

While the findings we have reviewed support the use of SV2A PET as an in vivo synaptic terminal marker, there are some issues that remain outstanding (Box 2). Additionally, we were unable to identify any research thus far to investigate the correlation between SV2A PET measures and measures of whole synapses (i.e., including postsynaptic components), so it remains unclear how closely SV2A measures are related to synaptic density, as opposed to presynaptic density. Another consideration is that altered binding of SV2A PET tracers may not be solely due to altered synaptic terminal density: alterations in SV2A copy number [132], or conformational changes in the protein itself affecting binding to tracer could affect the PET signal [133]. These issues could be addressed in future animal studies by combining in vivo PET imaging with ex vivo electron microscopy to count synapses and/or immunolabelling of pre- and postsynaptic protein markers in brain tissue. Human studies may also be feasible, particularly in neurodegenerative disorders where it may be possible to collect brain tissue postmortem. Additionally, the development of PET or other in vivo imaging measures of postsynaptic and glial markers that can be collected alongside SV2A PET data would provide a more complete picture of the synapse.

One issue relates to the reference region used in SV2A PET. The CSO has been widely used as a reference region in SV2A PET studies, however this comes with several caveats. Firstly, it is a white matter (WM) region, perfusion of which is less than half that of GM [134], leading to slower tracer delivery to WM relative to GM regions and a different time activity curve. Secondly, despite lacking synapses, the CSO does exhibit some specific binding of SV2A tracers [135], potentially leading to underestimation of GM DVR and BP_{ND}. This is observed in blocking studies with levetiracetam, which find post-blockade reductions in [^{11}C]UCB-J, [^{18}F]SynVesT-1 and [^{18}F]SynVesT-2 uptake in the CSO of 10–15%, 33.3% and 20% respectively [29, 35, 47], which would not be expected in a region lacking SV2A. It is unknown whether specific binding in the CSO may change with disease. Secondly, one study has estimated nondisplaceable uptake of [^{11}C]UCB-J in the CSO at around 20% higher than GM [135], due to differing lipid contents, which may explain the paradoxical observation that using the cerebellum, which is synaptically dense [136], as a reference region gives comparable group differences to results using the CSO [74, 77]. Use of the CSO may thus be further complicated in conditions associated with WM alterations, seen in depression [137], schizophrenia [138], bipolar disorder [139], neurodegenerative illness [140], and normal ageing [141]. Indeed, Holmes et al. noted lower CSO V_T in MDD versus controls [64]. The CSO should therefore be seen as a pseudoreference region [142], rather than a true reference region.

Studies in this review estimated either SUVR, BP_{ND}, DVR or V_T, advantages and limitations of which are described in Box 1. Most SV2A studies using BP_{ND} estimated this via the SRTM [57, 85–87, 89–91, 104], which rests on assumptions which are violated in SV2A PET (see Schizophrenia section), and which could negatively bias results and potentially overestimate group differences [59]. Many studies used SUVR. While SUVR values at 60–90 min correlate well with DVR measures [55, 143], these studies have been performed in healthy volunteers. In one blocking study, while SUVR showed good correlation with DVR-1 at baseline, it showed a negative bias of ~20% following levetiracetam [35] compared to DVR-1, cautioning that disease effects may affect SUVR differentially. SUVR is highly sensitive to inter-individual and -group variation in tracer uptake and delivery, as it does not utilise kinetic modelling. With DVR and V_T, the kinetic model allows estimation of tracer binding to the target at equilibrium. With SUVR, however, scans are taken within a predetermined time window after injection, meaning that variation in tracer kinetics cannot be accounted for. These factors introduce additional noise into the method, reducing power to detect changes. Indeed, use of quantitative outcome measures which allow for more sophisticated modelling has been shown to increase sensitivity [65]. In three cohorts which showed diverging results between studies, namely healthy aging, PD and MDD, this divergence was seen between studies using SUVR and those using V_T or other quantitative approaches as an outcome measure, with the SUVR studies reporting either nonsignificant or the more modest group differences than seen with the fully quantitative measures.

The limitations of different outcome measures should be considered when critically appraising studies, and future work to understand the expected impact of these issues on measured data and design solutions would be valuable. We do not recommend using SUVR as an outcome measure, as it is the outcome measure most subject to bias. Rather, BPND with the SRTM should be chosen if ABS is unavailable, ideally with explicit modelling of the CSO as a pseudoreference region [144]. DVR and BP_{ND} both require a suitable reference region, which has not been established for SV2A PET. We therefore recommend using VT with ABS where possible, although it should be recognised that it is subject to more noise than DVR and BP_{ND}.

Finally, SV2A's specificity for the synapse itself is not conclusive. Stockburger et al. [145] identified SV2A protein in isolated mitochondria in mice, including from outside the synapse, and found that SV2A knockdown altered mitochondrial morphology. These findings were replicated by Reichert [146], who estimates that 14.1% of SV2A colocalises with mitochondria throughout the cell, rather than being located in vesicles. They also found that mitochondrial stress, induced by the mitochondrial complex I inhibitor rotenone, promotes SV2A localisation in the mitochondrion, suggesting that [^{11}C]UCB-J PET studies in diseases also associated with mitochondrial dysfunction may show greater tracer uptake in mitochondria, which could potentially lead to underestimation of loss of SV2A from the synaptic terminal. Mitochondrial SV2A may also explain the specific binding in the CSO: WM does contain mitochondria [147].

Box 2. Outstanding issues for SV2A PET validation

1. Validation studies of PET measures of synaptic protein alongside in vitro quantification are scarce. Further studies are needed to determine relationships between PET measures of SV2A and other synaptic markers measured in vitro.
2. SV2A is a presynaptic marker. Further research investigating how changes in SV2A correlate with changes in the postsynaptic density and synaptic glia are need to give a more complete picture of synaptic alterations in neuropsychiatric disorders.
3. Blocking studies mostly use levetiracetam as the displacing ligand, which may underestimate the tracers' selectivity for the protein. Future blocking studies could use more selective ligands such as brivaracetam to further test selectivity.

Future research directions

SV2A is expressed in all synapses so far investigated, including GABAergic [148], glutamatergic [148], and dopaminergic [149] synapses. As such, SV2A PET imaging alone cannot determine whether alterations in a given disorder are in specific synapses or generalised. Multimodal imaging studies could help elucidate the specific synaptic changes seen in neuropsychiatric illness. For example, SV2A imaging combined with MRS, or PET studies of receptor density could provide information on whether synapses in certain neurotransmitter systems are differentially affected by a disease process. Other members of the SV2 family could be potential targets for the development of novel PET tracers, as expression of these proteins may be limited to subsets of GABAergic or glutamatergic synapses [150].

Evidence presented suggests that cognitive function shows relationships with SV2A measures across disorders, and there is limited evidence of a similar trend for ratings of depression and anxiety. It would be useful to investigate the contribution of social isolation, and other potential confounds, to SV2A findings. Combining datasets to investigate correlations of symptoms across disorders with SV2A imaging measures may be useful to investigate the role of synaptic mechanisms in the expression of symptoms across neuropsychiatric illness [151] and the contribution of social factors to imaging biomarkers and symptoms. In view of this, we recommend that future SV2A PET studies report data on social, cognitive and mood measures, even if not related to the core research question.

CONCLUSIONS

Four SV2A PET tracers with good reliability and high selectivity have been developed for human imaging to date. Studies using these tracers provide evidence that lower brain SV2A levels are associated with a number of neurological and psychiatric disorders relative to healthy controls, and with poorer cognitive function. The most replicated findings are in neurodegenerative illness, in particular tauopathies, where there is widespread lower tracer uptake relative to controls with large effect sizes in frontal cortex and hippocampus, as well as replicated findings in other regions. Amongst different psychiatric conditions studied to date, the hippocampus and PFC appear to be consistently implicated. Replicated findings in the ACC and frontal cortex are observed in chronic schizophrenia, but there are divergent findings earlier in the illness. Conflicting results are observed in major depression, although there are only two cross-sectional studies in patients of different age groups. More data is needed in both cohorts to determine whether there may be a different underlying neurobiology in later-life depression. Notwithstanding this, results from two studies suggest that drugs with antidepressant actions may increase SV2A levels. With the exception of Parkinson's disease, lower SV2A marker levels are generally associated with greater symptom severity, in particular cognitive dysfunction. It is possible that SV2A PET may be able to uncover synaptic mechanisms for certain symptoms across different diagnoses. Overall, findings are consistent with a crucial role for synapses in a broad range of neuropsychiatric conditions, and studies in aggregate point towards several promising directions, in terms of how synaptic imaging can help understand specific illnesses, but also the overlap between them.

REFERENCES

1. Bassett DS, Gazzaniga MS. Understanding complexity in the human brain. Trends Cogn Sci. 2011;15:200–9.
2. Lepeta K, Lourenco MV, Schweitzer BC, Martino Adami PV, Banerjee P, Catuara-Solarz S, et al. Synaptopathies: synaptic dysfunction in neurological disorders–A review from students to students. J Neurochem. 2016;138:785–805.
3. Wang X, Christian KM, Song H, Ming G-l. Synaptic dysfunction in complex psychiatric disorders: from genetics to mechanisms. Genome Med. 2018;10:1–3.
4. Calhoun ME, Jucker M, Martin LJ, Thinakaran G, Price DL, Mouton PR. Comparative evaluation of synaptophysin-based methods for quantification of synapses. J Neurocytol. 1996;25:821–8.
5. Petit TL, LeBoutillier JC. Quantifying synaptic number and structure: effects of stain and post-mortem delay. Brain Res. 1990;517:269–75.
6. Duric V, Banasr M, Stockmeier CA, Simen AA, Newton SS, Overholser JC, et al. Altered expression of synapse and glutamate related genes in post-mortem hippocampus of depressed subjects. Int J Neuropsychopharmacol. 2013;16:69–82.
7. McCluskey SP, Plisson C, Rabiner EA, Howes O. Advances in CNS PET: the state-of-the-art for new imaging targets for pathophysiology and drug development. Eur J Nucl Med Mol imaging. 2020;47:451–89.
8. Rossi R, Arjmand S, Bærentzen SL, Gjedde A, Landau AM. Synaptic vesicle glycoprotein 2A: features and functions. Front Neurosci. 2022;16:864514.
9. Visser M, O'Brien JT, Mak E. In vivo imaging of synaptic density in neurodegenerative disorders with positron emission tomography: A systematic review. Ageing Res Rev. 2024;94:102197.
10. Carson RE, Naganawa M, Toyonaga T, Koohsari S, Yang Y, Chen MK, et al. Imaging of synaptic density in neurodegenerative disorders. J Nucl Med. 2022;63:60S–67S.
11. Krnjević K. Chemical nature of synaptic transmission in vertebrates. Physiol Rev. 1974;54:418–540.
12. Citri A, Malenka RC. Synaptic plasticity: multiple forms, functions, and mechanisms. Neuropsychopharmacology 2008;33:18–41.
13. Di Maio V. The glutamatergic synapse: a complex machinery for information processing. Cogn Neurodyn. 2021;15:757–81. https://doi.org/10.1007/s11571-021-09679-w
14. Wimalasena K. Vesicular monoamine transporters: Structure-function, pharmacology, and medicinal chemistry. Medicinal Res Rev. 2011;31:483–519.
15. Brose N, Petrenko AG, Südhof TC, Jahn R. Synaptotagmin: a calcium sensor on the synaptic vesicle surface. Science. 1992;256:1021–5.
16. Pevsner J, Hsu S-C, Braun JE, Calakos N, Ting AE, Bennett MK, et al. Specificity and regulation of a synaptic vesicle docking complex. Neuron. 1994;13:353–61.
17. Cousin MA. Synaptophysin-dependent synaptobrevin-2 trafficking at the presynapse-Mechanism and function. J Neurochem. 2021;159:78–89.
18. Serrano ME, Kim E, Petrinovic MM, Turkheimer F, Cash D. Imaging synaptic density: the next holy grail of neuroscience? Front Neurosci. 2022;16:796129.
19. Varnäs K, Stepanov V, Halldin C. Autoradiographic mapping of synaptic vesicle glycoprotein 2A in non-human primate and human brain. Synapse. 2020;74:22157.
20. Nowack A, Yao J, Custer KL, Bajjalieh SM. SV2 regulates neurotransmitter release via multiple mechanisms. Am J Physiol-Cell Physiol. 2010;299:C960–7.
21. Innis RB, Cunningham VJ, Delforge J, Fujita M, Gjedde A, Gunn RN, et al. Consensus nomenclature for in vivo imaging of reversibly binding radioligands. J Cereb Blood Flow Metab. 2007;27:1533–9.
22. Lynch BA, Lambeng N, Nocka K, Kensel-Hammes P, Bajjalieh SM, Matagne A, et al. The synaptic vesicle protein SV2A is the binding site for the antiepileptic drug levetiracetam. Proc Natl Acad Sci. 2004;101:9861–6.
23. Cai H, Mangner T, Muzik O, Chugani H. Radiosynthesis and preliminary evaluation of 11C-levetiracetam for PET imaging of SV2A expression. Soc Nuclear Med. 2014; 55:1795.
24. Mercier J, Archen L, Bollu V, Carré S, Evrard Y, Jnoff E, et al. Discovery of heterocyclic nonacetamide synaptic vesicle protein 2A (SV2A) ligands with single-digit nanomolar potency: opening avenues towards the first SV2A positron emission tomography (PET) ligands. ChemMedChem. 2014;9:693–8.
25. Estrada S, Lubberink M, Thibblin A, Sprycha M, Buchanan T, Mestdagh N, et al. [11C] UCB-A, a novel PET tracer for synaptic vesicle protein 2 A. Nucl Med Biol. 2016;43:325–32.
26. Rabiner EA. Imaging synaptic density: a different look at neurologic diseases. J Nucl Med. 2018;59:380–1.
27. Nabulsi NB, Mercier J, Holden D, Carré S, Najafzadeh S, Vandergeten MC, et al. Synthesis and preclinical evaluation of 11C-UCB-J as a PET tracer for imaging the synaptic vesicle glycoprotein 2A in the brain. J Nucl Med. 2016;57:777–84.
28. Tuncel H, Boellaard R, Coomans EM, de Vries EF, Glaudemans AW, Feltes PK, et al. Kinetics and 28-day test–retest repeatability and reproducibility of [11C] UCB-J PET brain imaging. J Cereb Blood Flow Metab. 2021;41:1338–50.
29. Drake LR, Wu Y, Naganawa M, Asch R, Zheng C, Najafzadeh S, et al. First-in-Human Study of 18F-SynVesT-2: An SV2A PET Imaging Probe with Fast Brain Kinetics and High Specific Binding. J Nucl Med. 2024;65:462–9.
30. Cai Z, Drake L, Naganawa M, Najafzadeh S, Pracitto R, Lindemann M. et al. First-in-human study of [18F] SynVesT-2, a novel SV2A radioligand with fast kinetics and high specific binding signals. Soc Nuclear Med. 2020;61:462
31. Zheng C, Holden D, Zheng MQ, Pracitto R, Wilcox KC, Lindemann M, et al. A metabolically stable PET tracer for imaging synaptic vesicle protein 2A: synthesis and preclinical characterization of [18 F] SDM-16. Eur J Nucl Med Mol Imaging. 2022:1–15.
32. Tang Y, Liu P, Li W, Liu Z, Zhou M, Li J, et al. Detection of changes in synaptic density in amyotrophic lateral sclerosis patients using 18F-SynVesT-1 positron emission tomography. Eur J Neurol. 2022;29:2934–43.
33. Smart K, Uribe C, Desmond KL, Martin SL, Vasdev N, Strafella AP. Preliminary Assessment of Reference Region Quantification and Reduced Scanning Times for [18 F] SynVesT-1 PET in Parkinson's Disease. Mol Imaging. 2023;2023.
34. Li S, Naganawa M, Pracitto R, Najafzadeh S, Holden D, Henry S, et al. Assessment of test-retest reproducibility of [18 F] SynVesT-1, a novel radiotracer for PET imaging of synaptic vesicle glycoprotein 2A. Eur J Nucl Med Mol Imaging. 2021;48:1327–38.
35. Naganawa M, Li S, Nabulsi N, Henry S, Zheng MQ, Pracitto R, et al. First-in-human evaluation of 18F-SynVesT-1, a radioligand for PET imaging of synaptic vesicle glycoprotein 2A. J Nucl Med. 2021;62:561–7.
36. Löffler J, Herrmann H, Scheidhauer E, Wirth M, Wasserloos A, Solbach C, et al. Blocking studies to evaluate receptor-specific radioligand binding in the CAM model by PET and MR imaging. Cancers. 2022;14:3870.

37. Viviano M, Barresi E, Siméon FG, Costa B, Taliani S, Da Settimo F, et al. Essential Principles and Recent Progress in the Development of TSPO PET Ligands for Neuroinflammation Imaging. Curr Med Chem. 2022;29:4862–90. https://doi.org/10.2174/0929867329666220329204054
38. Kaminski RM, Gillard M, Klitgaard H. Targeting SV2A for discovery of antiepileptic drugs. 2012. In: Jasper's Basic Mechanisms of the Epilepsies [Internet]. 4th edition. Bethesda (MD): National Center for Biotechnology Information (US); 2012.
39. Cai H, Mangner TJ, Muzik O, Wang M-W, Chugani DC, Chugani HT. Radiosynthesis of 11C-levetiracetam: a potential marker for PET imaging of SV2A expression. ACS MedChem Lett. 2014;5:1152–5.
40. Lukyanetz E, Shkryl V, Kostyuk P. Selective blockade of N-type calcium channels by levetiracetam. Epilepsia. 2002;43:9–18.
41. Carunchio I, Pieri M, Ciotti MT, Albo F, Zona C. Modulation of AMPA receptors in cultured cortical neurons induced by the antiepileptic drug levetiracetam. Epilepsia. 2007;48:654–62.
42. Gillard M, Fuks B, Leclercq K, Matagne A. Binding characteristics of brivaracetam, a selective, high affinity SV2A ligand in rat, mouse and human brain: relationship to anti-convulsant properties. Eur J Pharmacol. 2011;664:36–44.
43. Warnock GI, Aerts J, Bahri MA, Bretin F, Lemaire C, Giacomelli F, et al. Evaluation of 18F-UCB-H as a novel PET tracer for synaptic vesicle protein 2A in the brain. J Nucl Med. 2014;55:1336–41.
44. Toyonaga T, Smith LM, Finnema SJ, Gallezot JD, Naganawa M, Bini J, et al. In vivo synaptic density imaging with 11C-UCB-J detects treatment effects of saracatinib in a mouse model of Alzheimer disease. J Nucl Med. 2019;60:1780–6.
45. Zheng C, Toyonaga T, Chen B, Nicholson L, Mennie W, Liu M, et al. Decreased synaptic vesicle glycoprotein A binding in a rodent model of familial Alzheimer's disease detected by [F] SDM. Cancer and Central Nervous System Disease Diagnosis and Treatment. 2023:136.
46. Sanchez-Varo R, Sanchez-Mejias E, Fernandez-Valenzuela JJ, De Castro V, Mejias-Ortega M, Gomez-Arboledas A, et al. Plaque-associated oligomeric amyloid-beta drives early synaptotoxicity in APP/PS1 mice hippocampus: ultrastructural pathology analysis. Front Neurosci. 2021;15:752594.
47. Finnema SJ, Nabulsi NB, Eid T, Detyniecki K, Lin SF, Chen MK, et al. Imaging synaptic density in the living human brain. Sci Transl Med. 2016;8:348ra96.
48. Thomsen MB, Schacht AC, Alstrup AKO, Jacobsen J, Lillethorup TP, Bærentzen SL, et al. Preclinical PET Studies of [11 C] UCB-J Binding in Minipig Brain. Mol Imaging Biol. 2020;22:1290–1300.
49. Smart K, Liu H, Matuskey D, Chen MK, Torres K, Nabulsi N, et al. Binding of the synaptic vesicle radiotracer [11C] UCB-J is unchanged during functional brain activation using a visual stimulation task. J Cereb Blood Flow Metab. 2021;41:1067–79.
50. Mansur A, Rabiner EA, Comley RA, Lewis Y, Middleton LT, Huiban M, et al. Characterization of 3 PET tracers for quantification of mitochondrial and synaptic function in healthy human brain: 18F-BCPP-EF, 11C-SA-4503, and 11C-UCB-J. J Nucl Med. 2020;61:96–103.
51. Toyonaga T, Khattar N, Wu Y, Lu Y, Naganawa M, Gallezot JD, et al. The regional pattern of age-related synaptic loss in the human brain differs from gray matter volume loss: in vivo PET measurement with [11C] UCB-J. Eur J Nucl Med Mol Imaging. 2023:1-11.
52. Fang XT, Volpi T, Holmes SE, Esterlis I, Carson RE, Worhunsky PD. Linking resting-state network fluctuations with systems of coherent synaptic density: A multimodal fMRI and 11C-UCB-J PET study. Front Hum Neurosci. 2023;17:1124254.
53. Michiels L, Delva A, van Aalst J, Ceccarini J, Vandenberghe W, Vandenbulcke M, et al. Synaptic density in healthy human aging is not influenced by age or sex: a 11C-UCB-J PET study. Neuroimage. 2021;232:117877.
54. Andersen KB, Hansen AK, Knudsen K, Schacht AC, Damholdt MF, Brooks DJ, et al. Healthy brain aging assessed with [18F] FDG and [11C] UCB-J PET. Nucl Med Biol. 2022;112:52–8.
55. Onwordi EC, Halff EF, Whitehurst T, Mansur A, Cotel MC, Wells L, et al. Synaptic density marker SV2A is reduced in schizophrenia patients and unaffected by antipsychotics in rats. Nat Commun. 2020;11:246.
56. Onwordi EC, Whitehurst T, Shatalina E, Mansur A, Arumuham A, Osugo M, et al. Synaptic Terminal Density Early in the Course of Schizophrenia: an in vivo UCB-J Positron Emission Tomographic Imaging Study of Synaptic Vesicle Glycoprotein 2A (SV2A). Biol Psychiatry 2023;S0006-3223:01353–7.
57. Yoon JH, Zhang Z, Mormino E, Davidzon G, Minzenberg MJ, Ballon J, et al. Reductions in synaptic marker SV2A in early-course Schizophrenia. J Psychiatr Res. 2023;161:213–7.
58. Radhakrishnan R, Skosnik PD, Ranganathan M, Naganawa M, Toyonaga T, Finnema S, et al. In vivo evidence of lower synaptic vesicle density in schizophrenia. Mol Psychiatry. 2021;26:7690–8.
59. Salinas CA, Searle GE, Gunn RN. The Simplified Reference Tissue Model: Model Assumption Violations and Their Impact on Binding Potential. J Cereb Blood Flow Metab. 2015;35:304–11. https://doi.org/10.1038/jcbfm.2014.202
60. Halff EF, Cotel M-C, Natesan S, McQuade R, Ottley CJ, Srivastava DP, et al. Effects of chronic exposure to haloperidol, olanzapine or lithium on SV2A and NLGN synaptic puncta in the rat frontal cortex. Behav Brain Res. 2021;405:113203.
61. Takaki M, Kodama M, Mizuki Y, Kawai H, Yoshimura B, Kishimoto M, et al. Effects of the antipsychotics haloperidol, clozapine, and aripiprazole on the dendritic spine. Eur Neuropsychopharmacol. 2018;28:610–9.
62. Gottschling C, Geissler M, Springer G, Wolf R, Juckel G, Faissner A. First and second generation antipsychotics differentially affect structural and functional properties of rat hippocampal neuron synapses. Neuroscience. 2016;337:117–30.
63. Casteele TV, Laroy M, Van Cauwenberge M, Koole M, Dupont P, Sunaert S, et al. 69. Lower Grey Matter Volume is not Related to Synaptic Density in Late Life Depression. Biol Psychiatry. 2023;93:S121–2.
64. Holmes SE, Scheinost D, Finnema SJ, Naganawa M, Davis MT, DellaGioia N, et al. Lower synaptic density is associated with depression severity and network alterations. Nat Commun. 2019;10:1529.
65. Doot RK, Kurland BF, Kinahan PE, Mankoff DA. Design considerations for using PET as a response measure in single site and multicenter clinical trials. Academic Radiol. 2012;19:184–90.
66. Holmes SE, Finnema SJ, Naganawa M, DellaGioia N, Holden D, Fowles K, et al. Imaging the effect of ketamine on synaptic density (SV2A) in the living brain. Mol Psychiatry. 2022;27:2273–81.
67. Asch RH, Holmes SE, Jastreboff AM, Potenza MN, Baldassarri SR, Carson RE, et al. Lower synaptic density is associated with psychiatric and cognitive alterations in obesity. Neuropsychopharmacology. 2022;47:543–52.
68. Angarita GA, Worhunsky PD, Naganawa M, Toyonaga T, Nabulsi NB, Li CR, et al. Lower prefrontal cortical synaptic vesicle binding in cocaine use disorder: An exploratory 11C-UCB-J positron emission tomography study in humans. Addiction Biol. 2022;27:13123.
69. D'souza DC, Radhakrishnan R, Naganawa M, Ganesh S, Nabulsi N, Najafzadeh S, et al. Preliminary in vivo evidence of lower hippocampal synaptic density in cannabis use disorder. Mol Psychiatry. 2021;26:3192–3200.
70. Hou J, Xiao Q, Zhou M, Xiao L, Yuan M, Zhong N, et al. Lower synaptic density associated with gaming disorder: an 18F-SynVesT-1 PET imaging study. General Psychiatry. 2023;36:e101112.
71. Huang YH, Lin Y, Mu P, Lee BR, Brown TE, Wayman G, et al. In vivo cocaine experience generates silent synapses. Neuron. 2009;63:40–7.
72. Lee BR, Ma Y-Y, Huang YH, Wang X, Otaka M, Ishikawa M, et al. Maturation of silent synapses in amygdala-accumbens projection contributes to incubation of cocaine craving. Nat Neurosci. 2013;16:1644–51.
73. Kalivas PW, Volkow ND. The neural basis of addiction: a pathology of motivation and choice. Am J Psychiatry. 2005;162:1403–13.
74. Chen M-K, Mecca AP, Naganawa M, Finnema SJ, Toyonaga T, Lin SF, et al. Assessing synaptic density in Alzheimer disease with synaptic vesicle glycoprotein 2A positron emission tomographic imaging. JAMA Neurol. 2018;75:1215–24.
75. Lu Y, Toyonaga T, Naganawa M, Gallezot JD, Chen MK, Mecca AP, et al. Partial volume correction analysis for 11C-UCB-J PET studies of Alzheimer's disease. Neuroimage. 2021;238:118248.
76. Chen M-K, Mecca AP, Naganawa M, Gallezot JD, Toyonaga T, Mondal J, et al. Comparison of [11C] UCB-J and [18F] FDG PET in Alzheimer's disease: a tracer kinetic modeling study. J Cereb Blood Flow Metab. 2021;41:2395–409.
77. Mecca AP, Chen MK, O'dell RS, Naganawa M, Toyonaga T, Godek TA, et al. In vivo measurement of widespread synaptic loss in Alzheimer's disease with SV2A PET. Alzheimer's Dement. 2020;16:974–82.
78. Bastin C, Bahri MA, Meyer F, Manard M, Delhaye E, Plenevaux A, et al. In vivo imaging of synaptic loss in Alzheimer's disease with [18F] UCB-H positron emission tomography. Eur J Nucl Med Mol imaging. 2020;47:390–402.
79. Vanderlinden G, Ceccarini J, Vande Casteele T, Michiels L, Lemmens R, Triau E, et al. Spatial decrease of synaptic density in amnestic mild cognitive impairment follows the tau build-up pattern. Mol Psychiatry. 2022;27:4244–51.
80. Vanhaute H, Ceccarini J, Michiels L, Koole M, Sunaert S, Lemmens R, et al. In vivo synaptic density loss is related to tau deposition in amnestic mild cognitive impairment. Neurology. 2020;95:e545–53.
81. Venkataraman AV, Bishop C, Mansur A, Rizzo G, Lewis Y, Kocagoncu E. et al. Imaging synaptic microstructure and synaptic loss in vivo in early Alzheimer's Disease. medRxiv. 2021. https://doi.org/10.1101/2021.11.23.21266746.
82. Zhang J, Wang J, Xu X, You Z, Huang Q, Huang Y, et al. In vivo synaptic density loss correlates with impaired functional and related structural connectivity in Alzheimer's disease. J Cereb Blood Flow Metab. 2023;43:977–88.
83. Moallemian S, Salmon E, Bahri MA, Beliy N, Delhaye E, Balteau E, et al. Multimodal imaging of microstructural cerebral alterations and loss of synaptic density in Alzheimer's disease. Neurobiol Aging. 2023;132:24–35.
84. O'Dell RS, Mecca AP, Chen MK, Naganawa M, Toyonaga T, Lu Y, et al. Association of Aβ deposition and regional synaptic density in early Alzheimer's disease: a

PET imaging study with [11 C] UCB-J. Alzheimer's Research & Therapy. 2021;13:1–2.
85. Holland N, Malpetti M, Rittman T, Mak EE, Passamonti L, Kaalund SS, et al. Molecular pathology and synaptic loss in primary tauopathies: an 18F-AV-1451 and 11C-UCB-J PET study. Brain. 2022;145:340–8.
86. Holland N, Jones PS, Savulich G, Wiggins JK, Hong YT, Fryer TD, et al. Synaptic loss in primary tauopathies revealed by [11C] UCB-J positron emission tomography. Mov Disord. 2020;35:1834–42.
87. Mak E, Holland N, Jones PS, Savulich G, Low A, Malpetti M, et al. In vivo coupling of dendritic complexity with presynaptic density in primary tauopathies. Neurobiol Aging. 2021;101:187–98.
88. Salmon E, Bahri MA, Plenevaux A, Becker G, Seret A, Delhaye E, et al. In vivo exploration of synaptic projections in frontotemporal dementia. Sci Rep. 2021;11:16092.
89. Malpetti M, Jones PS, Cope TE, Holland N, Naessens M, Rouse MA, et al. Synaptic Loss in Frontotemporal Dementia Revealed by [11C] UCB-J Positron Emission Tomography. Ann Neurol. 2023;93:142–54.
90. Whiteside DJ, Holland N, Tsvetanov KA, Mak E, Malpetti M, Savulich G, et al. Synaptic density affects clinical severity via network dysfunction in syndromes associated with frontotemporal lobar degeneration. Nat Commun. 2023;14:8458.
91. Holland N, Jones PS, Savulich G, Naessens M, Malpetti M, Whiteside DJ, et al. Longitudinal Synaptic Loss in Primary Tauopathies: An In Vivo [11C] UCB-J Positron Emission Tomography Study. Mov Disord. 2023;38:1316–1326.
92. Dickson DW, Kouri N, Murray ME, Josephs KA. Neuropathology of frontotemporal lobar degeneration-tau (FTLD-tau). J Mol Neurosci. 2011;45:384–9.
93. Matuskey D, Tinaz S, Wilcox KC, Naganawa M, Toyonaga T, Dias M, et al. Synaptic changes in Parkinson disease assessed with in vivo imaging. Ann Neurol. 2020;87:329–38.
94. Delva A, Van Weehaeghe D, Koole M, Van Laere K, Vandenberghe W. Loss of presynaptic terminal integrity in the substantia nigra in early Parkinson's disease. Mov Disord. 2020;35:1977–86.
95. Wilson H, Pagano G, de Natale ER, Mansur A, Caminiti SP, Polychronis S, et al. Mitochondrial complex 1, sigma 1, and synaptic vesicle 2A in early drug-naive Parkinson's disease. Mov Disord. 2020;35:1416–27.
96. Andersen KB, Hansen AK, Schacht AC, Horsager J, Gottrup H, Klit H, et al. Synaptic Density and Glucose Consumption in Patients with Lewy Body Diseases: An [11C] UCB-J and [18F] FDG PET Study. Mov Disord. 2023;38:796–805
97. Delva A, Van Laere K, Vandenberghe W. Longitudinal positron emission tomography imaging of presynaptic terminals in early Parkinson's disease. Mov Disord. 2022;37:1883–92.
98. Andersen KB, Hansen AK, Damholdt MF, Horsager J, Skjaerbaek C, Gottrup H, et al. Reduced synaptic density in patients with lewy body dementia: An [11C] UCB-J PET imaging study. Mov Disord. 2021;36:2057–65.
99. Van Cauwenberge MGA, Delva A, Vande Casteele T, Laroy M, Radwan A, Vansteelandt K, et al. Mild Motor Signs in Healthy Aging Are Associated with Lower Synaptic Density in the Brain. Mov Disord. 2023;38:1786–94.
100. Hanganu A, Bedetti C, Degroot C, Mejia-Constain B, Lafontaine AL, Soland V, et al. Mild cognitive impairment is linked with faster rate of cortical thinning in patients with Parkinson's disease longitudinally. Brain. 2014;137:1120–9.
101. Delva A, Michiels L, Koole M, Van Laere K, Vandenberghe W. Synaptic damage and its clinical correlates in people with early Huntington disease: a PET study. Neurology. 2022;98:e83–94.
102. Delva A, Van Laere K, Vandenberghe W. Longitudinal Imaging of Regional Brain Volumes, SV2A, and Glucose Metabolism In Huntington's Disease. Mov Disord. 2023;38:1515–26.
103. Mecca AP, O'dell RS, Sharp ES, Banks ER, Bartlett HH, Zhao W, et al. Synaptic density and cognitive performance in Alzheimer's disease: A PET imaging study with [11C] UCB-J. Alzheimer's Dement. 2022;18:2527–36.
104. Nicastro N, Holland N, Savulich G, Carter SF, Mak E, Hong YT, et al. 11C-UCB-J synaptic PET and multimodal imaging in dementia with Lewy bodies. Eur J hybrid imaging. 2020;4:1–7.
105. Yanamandra K, Jiang H, Mahan TE, Maloney SE, Wozniak DF, Diamond MI, et al. Anti-tau antibody reduces insoluble tau and decreases brain atrophy. Ann Clin Transl Neurol. 2015;2:278–88.
106. Howes OD, Cummings C, Chapman GE, Shatalina E. Neuroimaging in schizophrenia: an overview of findings and their implications for synaptic changes. Neuropsychopharmacology. 2023;48:151–67.
107. Zhang H, Schneider T, Wheeler-Kingshott CA, Alexander DC. NODDI: practical in vivo neurite orientation dispersion and density imaging of the human brain. Neuroimage. 2012;61:1000–16.
108. Onwordi EC, Whitehurst T, Mansur A, Statton B, Berry A, Quinlan M, et al. The relationship between synaptic density marker SV2A, glutamate and N-acetyl aspartate levels in healthy volunteers and schizophrenia: a multimodal PET and magnetic resonance spectroscopy brain imaging study. Transl Psychiatry. 2021;11:393. https://doi.org/10.1038/s41398-021-01515-3
109. Puts NA, Edden RA. In vivo magnetic resonance spectroscopy of GABA: a methodological review. Prog Nucl Magn Reson Spectrosc. 2012;60:29–41.
110. Mecca AP, Chen M-K, O'dell RS, Naganawa M, Toyonaga T, Godek TA, et al. Association of entorhinal cortical tau deposition and hippocampal synaptic density in older individuals with normal cognition and early Alzheimer's disease. Neurobiol Aging. 2022;111:44–53.
111. Coomans EM, Schoonhoven DN, Tuncel H, Verfaillie SCJ, Wolters EE, Boellaard R, et al. In vivo tau pathology is associated with synaptic loss and altered synaptic function. Alzheimer's Res Ther. 2021;13:1–13.
112. Kopeikina KJ, Polydoro M, Tai HC, Yaeger E, Carlson GA, Pitstick R, et al. Synaptic alterations in the rTg4510 mouse model of tauopathy. J Comp Neurol. 2013;521:1334–53.
113. Jackson JS, Witton J, Johnson JD, Ahmed Z, Ward M, Randall AD, et al. Altered synapse stability in the early stages of tauopathy. Cell Rep. 2017;18:3063–8.
114. Dejanovic B, Huntley MA, De Mazière A, Meilandt WJ, Wu T, Srinivasan K, et al. Changes in the synaptic proteome in tauopathy and rescue of tau-induced synapse loss by C1q antibodies. Neuron. 2018;100:1322–36.e7.
115. Yoshiyama Y, Higuchi M, Zhang B, Huang SM, Iwata N, Saido TC, et al. Synapse loss and microglial activation precede tangles in a P301S tauopathy mouse model. Neuron 2007;53:337–51.
116. Finnema SJ, Toyonaga T, Detyniecki K, Chen MK, Dias M, Wang Q, et al. Reduced synaptic vesicle protein 2A binding in temporal lobe epilepsy: A [11C] UCB-J positron emission tomography study. Epilepsia. 2020;61:2183–93.
117. Harris JJ, Jolivet R, Attwell D. Synaptic energy use and supply. Neuron. 2012;75:762–77.
118. Faria-Pereira A, Morais VA. Synapses: The brain's energy-demanding sites. Int J Mol Sci. 2022;23:3627.
119. Mattson MP, Pedersen WA, Duan W, Culmsee C, Camandola S. Cellular and molecular mechanisms underlying perturbed energy metabolism and neuronal degeneration in Alzheimer's and Parkinson's diseases. Ann N. Y Acad Sci. 1999;893:154–75.
120. Godsil BP, Kiss JP, Spedding M, Jay TM. The hippocampal–prefrontal pathway: The weak link in psychiatric disorders? Eur Neuropsychopharmacol. 2013;23:1165–81.
121. Sigurdsson T, Duvarci S. Hippocampal-prefrontal interactions in cognition, behavior and psychiatric disease. Front Syst Neurosci. 2016;9:190.
122. Schultz W. Reward functions of the basal ganglia. J Neural Transm. 2016;123:679–93.
123. Moyer CE, Shelton MA, Sweet RA. Dendritic spine alterations in schizophrenia. Neurosci Lett. 2015;601:46–53.
124. Nakamura H, Kobayashi S, Ohashi Y, Ando S. Age-changes of brain synapses and synaptic plasticity in response to an enriched environment. J Neurosci Res. 1999;56:307–15.
125. Wang H, Xu X, Xu X, Gao J, Zhang T. Enriched environment and social isolation affect cognition ability via altering excitatory and inhibitory synaptic density in mice hippocampus. Neurochem Res. 2020;45:2417–32.
126. Rayner G, Jackson G, Wilson S. Cognition-related brain networks underpin the symptoms of unipolar depression: evidence from a systematic review. Neurosci Biobehav Rev. 2016;61:53–65.
127. Xu J, Van Dam NT, Feng C, Luo Y, Ai H, Gu R, et al. Anxious brain networks: A coordinate-based activation likelihood estimation meta-analysis of resting-state functional connectivity studies in anxiety. Neurosci Biobehav Rev. 2019;96:21–30.
128. Wang X, Chang Z, Wang R. Opposite effects of positive and negative symptoms on resting-state brain networks in schizophrenia. Commun Biol. 2023;6:279.
129. Wang R, Liu M, Cheng X, Wu Y, Hildebrandt A, Zhou C. Segregation, integration, and balance of large-scale resting brain networks configure different cognitive abilities. Proc Natl Acad Sci. 2021;118:e2022288118.
130. Holmes SE, Abdallah C, Esterlis I. Imaging synaptic density in depression. Neuropsychopharmacology. 2023;48:186–90.
131. Elger CE, Grunwald T, Lehnertz K, Kutas M, Helmstaedter C, Brockhaus A, et al. Human temporal lobe potentials in verbal learning and memory processes. Neuropsychologia. 1997;35:657–67.
132. De Wilde MC, Overk CR, Sijben JW, Masliah E. Meta-analysis of synaptic pathology in Alzheimer's disease reveals selective molecular vesicular machinery vulnerability. Alzheimer's Dement. 2016;12:633–44.
133. Ramos-Miguel A, Jones AA, Petyuk VA, Barakauskas VE, Barr AM, Leurgans SE, et al. Proteomic identification of select protein variants of the SNARE interactome associated with cognitive reserve in a large community sample. Acta Neuropathol. 2021;141:755–70.
134. Parkes LM, Rashid W, Chard DT, Tofts PS. Normal cerebral perfusion measurements using arterial spin labeling: reproducibility, stability, and age and gender effects. Magn Reson Med. 2004;51:736–43.

135. Rossano S, Toyonaga T, Finnema SJ, Naganawa M, Lu Y, Nabulsi N, et al. Assessment of a white matter reference region for 11C-UCB-J PET quantification. J Cereb Blood Flow Metab. 2020;40:1890–901.
136. Napper R, Harvey R. Number of parallel fiber synapses on an individual Purkinje cell in the cerebellum of the rat. J Comp Neurol. 1988;274:168–77.
137. Wang L, Leonards CO, Sterzer P, Ebinger M. White matter lesions and depression: a systematic review and meta-analysis. J Psychiatr Res. 2014;56:56–64.
138. Davis KL, Stewart DG, Friedman JI, Buchsbaum M, Harvey PD, Hof PR, et al. White matter changes in schizophrenia: evidence for myelin-related dysfunction. Arch Gen Psychiatry. 2003;60:443–56.
139. Mahon K, Burdick KE, Szeszko PR. A role for white matter abnormalities in the pathophysiology of bipolar disorder. Neurosci Biobehav Rev. 2010;34:533–54.
140. Nasrabady SE, Rizvi B, Goldman JE, Brickman AM. White matter changes in Alzheimer's disease: a focus on myelin and oligodendrocytes. Acta Neuropathol Commun. 2018;6:1–10.
141. Barrick TR, Charlton RA, Clark CA, Markus HS. White matter structural decline in normal ageing: a prospective longitudinal study using tract-based spatial statistics. Neuroimage. 2010;51:565–77.
142. Mansur A. Quantitative imaging of mitochondrial and synaptic function in the human brain with 18F-BCPP-EF, 11C-SA-4503, and 11C-UCB-J. Imperial College London. 2020.
143. Koole M, van Aalst J, Devrome M, Mertens N, Serdons K, Lacroix B, et al. Quantifying SV2A density and drug occupancy in the human brain using [11 C] UCB-J PET imaging and subcortical white matter as reference tissue. Eur J Nucl Med Mol imaging. 2019;46:396–406.
144. Gunn RN, Murthy V, Catafau AM, Searle G, Bullich S, Slifstein M, et al. Translational characterization of [11C] GSK931145, a PET ligand for the glycine transporter type 1. Synapse. 2011;65:1319–32.
145. Stockburger C, Miano D, Baeumlisberger M, Pallas T, Arrey TN, Karas M, et al. A mitochondrial role of SV2a protein in aging and Alzheimer's disease: studies with levetiracetam. J Alzheimer's Dis. 2016;50:201–15.
146. Reichert JS. SV2A-just a synaptic vesicle protein? Unravelling the interaction of SV2A and mitochondria in the pathogenesis and therapy of Morbus Alzheimer. Dissertation, Mainz, Johannes Gutenberg-Universität Mainz, 2022;2022.
147. Stahon KE, Bastian C, Griffith S, Kidd GJ, Brunet S, Baltan S. Age-related changes in axonal and mitochondrial ultrastructure and function in white matter. J Neurosci. 2016;36:9990–10001.
148. Pazarlar BA, Aripaka SS, Petukhov V, Pinborg L, Khodosevich K, Mikkelsen JD. Expression profile of synaptic vesicle glycoprotein 2A, B, and C paralogues in temporal neocortex tissue from patients with temporal lobe epilepsy (TLE). Mol Brain. 2022;15:1–10.
149. Vanoye-Carlo A, Gómez-Lira G. Differential expression of SV2A in hippocampal glutamatergic and GABAergic terminals during postnatal development. Brain Res. 2019;1715:73–83.
150. Bartholome O, Van den Ackerveken P, Sánchez Gil J, de la Brassinne Bonardeaux O, Leprince P, Franzen R, et al. Puzzling out synaptic vesicle 2 family members functions. Front Mol Neurosci. 2017;10:148.
151. Ross CA, Margolis RL. Research domain criteria: strengths, weaknesses, and potential alternatives for future psychiatric research. Complex Psychiatry. 2019;5:218–36.
152. Pracitto R, Wilcox KC, Lindemann M, Tong J, Zheng C, Li S, et al. Further Investigation of Synaptic Vesicle Protein 2A (SV2A) Ligands Designed for Positron Emission Tomography and Single-Photon Emission Computed Tomography Imaging: Synthesis and Structure–Activity Relationship of Substituted Pyridinylmethyl-4-(3, 5-difluorophenyl) pyrrolidin-2-ones. ACS Omega. 2021;6:27676–83.
153. Patel S, Knight A, Krause S, Teceno T, Tresse C, Li S, et al. Preclinical in vitro and in vivo characterization of synaptic vesicle 2A–targeting compounds amenable to F-18 labeling as potential PET radioligands for imaging of synapse integrity. Mol Imaging Biol. 2020;22:832–41.
154. Finnema SJ, Nabulsi NB, Mercier J, Lin SF, Chen MK, Matuskey D, et al. Kinetic evaluation and test–retest reproducibility of [11 C] UCB-J, a novel radioligand for positron emission tomography imaging of synaptic vesicle glycoprotein 2 A in humans. J Cereb Blood Flow Metab. 2018;38:2041–52.
155. Bahri MA, Plenevaux A, Aerts J, Bastin C, Becker G, Mercier J, et al. Measuring brain synaptic vesicle protein 2 A with positron emission tomography and [18 F] UCB-H. Alzheimer's Dement: Transl Res Clin Interventions. 2017;3:481–6.
156. Bretin F, Bahri MA, Bernard C, Warnock G, Aerts J, Mestdagh N, et al. Biodistribution and radiation dosimetry for the novel SV2A radiotracer [18 F] UCB-H: first-in-human study. Mol imaging Biol. 2015;17:557–64.
157. Cai Z, Wu Y, Drake L, Naganawa M, Najafzadeh S, Pracitto R, et al. Evaluation of [18 F] SynVesT-2 for imaging SV2A in the human brain: kinetics, test-retest reproducibility, and binding specificity. Soc Nuclear Med. 2021;62:44.
158. Bertoglio D, Verhaeghe J, Miranda A, Kertesz I, Cybulska K, Korat Š, et al. Validation and noninvasive kinetic modeling of [11 C] UCB-J PET imaging in mice. J Cereb Blood Flow Metab. 2020;40:1351–62.
159. Serrano ME, Becker G, Bahri MA, Seret A, Mestdagh N, Mercier J, et al. Evaluating the in vivo specificity of [18 F] UCB-H for the SV2A protein, compared with SV2B and SV2C in rats using microPET. Molecules 2019;24:1705.
160. Bertoglio D, Zajicek F, Lombaerde S, Miranda A, Stroobants S, Wang Y, et al. Validation, kinetic modeling, and test-retest reproducibility of [18 F] SynVesT-1 for PET imaging of synaptic vesicle glycoprotein 2 A in mice. J Cereb Blood Flow Metab. 2022;42:1867–78.
161. Lammertsma AA, Hume SP. Simplified reference tissue model for PET receptor studies. Neuroimage. 1996;4:153–8.
162. Chen Z, Liao G, Wan N, He Z, Chen D, Tang Z, et al. Synaptic loss in spinocerebellar ataxia type 3 revealed by SV2A positron emission tomography. Movement Disorders. 2023;38:978–89.

AUTHOR CONTRIBUTIONS

RC and JM contributed to literature search, data extraction for tables, and writing the manuscript. OH conceptualised and contributed to writing the manuscript. FET reviewed and provided feedback. All authors provided approval before submission.

FUNDING

For the purpose of open access, this paper has been published under a creative common licence (CC-BY) to any accepted author manuscript version arising from this submission. This study was funded by Medical Research Council-UK (MC_U120097115; MR/W005557/1 and MR/V013734/1), and Wellcome Trust (no. 094849/Z/10/Z) grants to OH and the National Institute for Health and Care Research (NIHR) Biomedical Research Centre at South London and Maudsley NHS Foundation Trust and King's College London. The views expressed are those of the author(s) and not necessarily those of the NIHR or the Department of Health.

COMPETING INTERESTS

OH has received investigator-initiated research funding from and/or participated in advisory/speaker meetings organised by Angellini, Autifony, Biogen, Boehringer-Ingelheim, Eli Lilly, Elysium, Heptares, Global Medical Education, Invicro, Jansenn, Karuna, Lundbeck, Merck, Neurocrine, Ontrack/ Pangea, Otsuka, Sunovion, Recordati, Roche, Rovi and Viatris/Mylan. He was previously a part-time employee of Lundbeck A/v. OH has a patent for the use of dopaminergic imaging. RC, FET and JM have no competing interests to declare.

ADDITIONAL INFORMATION

Supplementary information The online version contains supplementary material available at https://doi.org/10.1038/s41386-024-01943-x.

Correspondence and requests for materials should be addressed to Oliver Howes.

Reprints and permission information is available at http://www.nature.com/reprints

Publisher's note Springer Nature remains neutral with regard to jurisdictional claims in published maps and institutional affiliations.